# Determination of the local viscosity inside polymerizing particles in emulsion via polarized fluorescence spectroscopy

**Dissertation**

**Submitted for the acquisition of a PhD degree in natural sciences**

by

Msc. Bertrand Xavier Takam Mangoua

from Nkongsamba / Cameroon

Approved by

the faculty of Mathematics and Natural sciences

of the Clausthal University of Technology

day of examination:

20.12.2002

This thesis was undertaken at the Institute of physical chemistry of the Clausthal University of Technology.

Dean: Prof. Dr. phil. nat. J. Fertig

Supervisor: P.D. Dr. J. Adams

Co-supervisor: Prof. Dr. J. Fuhrmann and

Prof. Dr. Alex M. van Herk (TU Eindhoven)

## Eidesstattliche Erklärungen

Hiermit erkläre ich an Eides statt, dass ich die vorgelegte Arbeit selbständig, ohne unerlaubte Hilfe verfasst und die benutzten Hilfsmittel vollständig angegeben habe.

Hiermit erkläre ich an Eides statt, dass ich noch keine früheren Promotionsversuche unternommen habe.

Bertrand Takam Mangoua

**Abstract**

In heterogeneous reaction mixtures like an emulsion, it is important to determine thermodynamic and dynamic properties not only for the whole system, but also scaled down to the sizes of the heterogeneous structures. Among others fluorescence techniques belong to the methods allowing the study of a great variety of phenomena occurring in such systems. Advantages of fluorescence are the high sensitivity, the possibility of probe delegation and the easy accessibility of the ns-time scale for dynamical investigations. By the appropriate choice of the fluorescence probe, fluorescence can be used for example to give an insight into kinetic aspects of an emulsion polymerization.

My thesis addresses the application of the fluorescence depolarization technique to solve relevant problems in polymerization system, notably the investigation of the local viscosity inside a polymerizing particle. The viscosity of the whole system changes marginally during the polymerization while the local viscosity inside the polymerization particle changes drastically. The local viscosity was derived from the fluorescence anisotropy *r*, which is linked to the rotational mobility of the fluorescence probe.

For the experiments of the present work, perylene was used as fluorescence probe. This probe is soluble only in the oil phase of the investigated styrene/water micro-emulsion. This system was chosen, because it is transparent at the beginning of the polymerization and shows a relatively low turbidity after the reaction. Turbidity is a major problem for the investigation of emulsion polymerization with polarized light: in a turbid medium multiple scattering of the excitation and fluorescence photons occurs, leading to a reduction of the anisotropy and thus too low values of the viscosity.

To obtain the desired correct micro-viscosity inside the particle a correction method, which accounts for the influence of multiple scattering on the

fluorescence anisotropy, was applied. To achieve this goal, the polarized intensities of purely scattered light at the fluorescence excitation and emission wavelength were recorded together with the fluorescence intensities.

The corrected anisotropy and thus the microviscosity shows a relatively fast (~10 min) increase to a constant value. However, the also determined degree of conversion (measured online via dilatometer) increases typically for another 20 mins before the polymerization is completed. A comparison of the conversion and the particle size leads to the observation that the size of the particle changes very little during the process.

The results of the thesis clearly demonstrate that the fluorescence depolarization technique is a good tool for the investigation of the local properties of a polymerizing emulsion system. Moreover, combined with dilatometer, it also gives the opportunity to investigate kinetic parameters of the process.

## Table of contents

To:

My parents Dominique and Marguerite Mangoua

My wife Charity Takam

**Acknowledgements**

I will first of all like to thank Pr. Dr. J. Fuhrmann for offering me the possibility to join his research group and for his advice, encouragement and any stimulating discussions.

I also thank my supervisors Priv.-Doz. Dr. J. Adams and Prof. Dr. A. Herk for their advice and availability. I am greatly indebted to Dr. Adams for many valuable suggestions and for his constant interest in this work and also his readiness for discussion.

Special thanks goes to my friend Dr. E. Suh and my wife Charity for going through the manuscripts. I also thank the supervisors of the European Graduate School (EGS) on the „Microstructural Control In Free-Radical Polymerization“ for their comments.

I will like to thank the present and the former members of the institute of physical chemistry (TU Clausthal) for the friendly and pleasant work climate they created in this institute and, which contributed to encourage me; specially M. Dehnke for his help during AFM measurements and Dr. Rynka my “ German teacher”.

I also thank the PhD students of the EGS especially those of Eindhoven for their help during my stay in the group of Prof. Dr. A. Herk.

The last but not the least I will like to thank all the members of my family especially Mr Djoko Michel, Ms Djoko Julienne, Dr. Fotsing Mangoua for their moral support and encouragement. Special thanks also goes to my friends Cheussom Levis, Dr. Paul Woafo and to those whose names have not been mention.

This work was supported by DFG through the EGS

# 1. Introduction and objective of the thesis

Microemulsions are macroscopically homogeneous mixtures of oil, water and surfactant, which on the microscopic level consist of individual domains of oil and water separated by a monolayer of amphiphile[1]. They are isotropic, optically transparent or translucent and thermodynamically stable.

In contrast to emulsion polymerization[2-5], polymerization in microemulsion is a relatively new polymerization technique, which allows the preparation of ultrafine latex particles. Nevertheless, a number of studies have appeared reporting experimental results for the polymerization mechanism and kinetic[6-9]. In these studies, it is pointed out that the particle nucleation occurs in monomer-swollen micelles and finally initiates the polymerization therein. The chain stopping event in the actives polymerizing particles are the chain transfer reactions to monomer and radical desorption from the polymer particle. The particle sizes change very little during the course of the polymerization and very high molecular weight can be achieved[10-12].

Less attention has been given to the physical changes, particularly to the change of the local viscosity, occurring within these polymerizing particles during the course of the reaction. It has been shown that during the polymerization process the viscosity of the system increases. High viscosity affects the termination reactions since they are diffusion-controlled. When the viscosity of the medium is high, extensive entanglements hinder the movement of the polymer chains. This leads to the well-known Trommsdorff-Norrish effect[13]. Since the motion of the reaction species (monomer, radical, chain…) are diffusion-controlled and the diffusion itself is affected by viscosity, it is thus interesting to investigate the behavior of the viscosity at molecular level.

Several techniques have been used to get more insight to the kinetics of microemulsion polymerization and to investigate various microscopic processes

occurring at the loci of polymerization[14-20]. None of these was able to look very closely at the change of the local viscosity within the polymerizing particles.

The main objective of this thesis is to apply fluorescence depolarization technique as an online method to monitor the change of local viscosity. The local viscosity is defined here as the viscosity at the loci where the polymerization takes place. It should not be confused with the bulk viscosity of the system: they behave differently. The microviscosity of a polymer system is obtained by measuring the mobility of a small probe trapped in it. In contrast to the macroviscisity, which gives insight to the flow of the entire polymer chain, the local or microviscosity gives information about the scale of the probe order i.e. dimension of a few Å. Thus the probe mobility is influenced only by a short section of the polymer, i.e. one or few monomer segments and not the entire chain. Using fluorescence depolarization technique will lead to an average local viscosity since only an average mobility of the probe can be determined.

The performances of fluorescence spectroscopy[21-26] depend to a large extent on the properties of the fluorescent probe employed. The principle of determination of the local viscosity during emulsion polymerization using this technique is known and has been already applied by Chung[27]. Using sodium salt of pyrene tetrasulfonic acid (PTA) as fluorescence probe, online and offline-polarized fluorescence were applied by Chung[27] to investigate the inverse microemulsion polymerization of acrylamide. She related some aspects of the inverse microemulsion polymerization mechanism to the behavior of PTA during the polymerization process. In contrast to the work of Chung where a transparent system was used (inverse microemulsion), a turbid system is investigated here. The system under investigation is a polymerizing microemulsion of styrene in water. The turbidity of this system changes slightly with time leading to a different behavior compared to that investigated by Chung.

In order to use fluorescence depolarization as a molecular level viscosimeter, an appropriate fluorescent dye has to be considered. In the following work,

perylene is chosen for this purpose. The change of the local viscosity will be determined and correlated to the overall conversion of monomer to polymer measured simultaneously by a dilatometer. The technique is not straightforward since during the polymerization, the transparent microemulsion becomes slightly turbid leading to the multiple scattering that decreases the observed anisotropy of fluorescence. A correction of this anisotropy will be needed before the evaluation of the change of the local viscosity.

# 2. Polymerization technique

The basic knowledge on emulsion polymerization[31-39] is used as fundaments for the studies of the polymerization in microemulsion. This polymerization system in some aspects is very close to emulsion polymerization. The difference resides in the physical state of the microemulsion. In microemulsion systems the use of co-surfactant is needed, no monomer droplet exists, and the system is translucent.

## 2.1. Microemulsion

Microemulsions are thermodynamically stable, transparent or translucent dispersions consisting of very small droplets with radii of order of 5 – 15 nm. The main components of microemulsion are: oil, water, surfactant and co-surfactant. A surfactant molecule is a molecule having both hydrophilic and hydrophobic group in its molecular structure. When dissolved in water and above the critical micelle concentration (*cmc*) surfactant molecules aggregate and form micelles with different sizes and shapes[1].

When oil and water are mixed with relatively large amount of surfactant and co-surfactant, microemulsions are obtained spontaneously, either in the form of water in oil (w/o), or oil in water (o/w), or bicontinuous structure in which aqueous and oily domains are interconnected. The oil in water (o/w) microemulsion is obtained when oil, usually, the monomer, is dispersed in water. If oil is the continuous phase and water the dispersing medium, then the system is the inverse microemulsion or water in oil microemulion. The surfactant usually distributes itself between water and the interface whereas the co-surfactant partitions between the oil phase and the interface. The co-surfactant, usually a short chain alcohol, plays several roles in the system among which is the reduction of the lifetime of surfactant molecule inside a micelle. Surfactants aggregation is diffusion-controlled and the presence of alcohol as

co-surfactant thus reduces the size of the aggregates by lowering the interfacial tension.

The choice of the surfactant is decisive for the preparation of microemulsion. Not only the hydrophilic-hydrophobic balance has to be taken into account but also the geometry of the molecule. The packing property of a surfactant depends on their head group area, on the hydrocarbon volume, and the extend-length of the surfactant hydrophobic chain. It is from these geometrical considerations that surfactants with moderately long straight-chain aliphatic tails are considered most suitable for the preparation of o/w microemulsion, surfactants with rather bulky hydrophobic chains are good for bicountinuous microemulsion, and surfactants with highly branched hydrophobic tails should be used for w/o microemulsion[1]. Often a combination of surfactants is used in the formulation.

The properties of microemulsion are independent of time and they return to their initial state when subjected to a small disturbance, which is subsequently relaxed. Figure 2.1 shows schematically the phase behavior of water, surfactant and oil system at fixed temperature and pressure[1]. There is a very strong segregation into three domains: oil and water domains and surfactant monolayer films. The shapes of microemulsion particles change from one domain to another but the size of the droplets remains constant[1]. A microemulsion phase may be in equilibrium with excess oil (Winsor I or lower phase of microemulsion), with excess water (Winsor II or upper phase of microemulsion), or with both excess phases (Winsor III or middle phase of microemulsion).

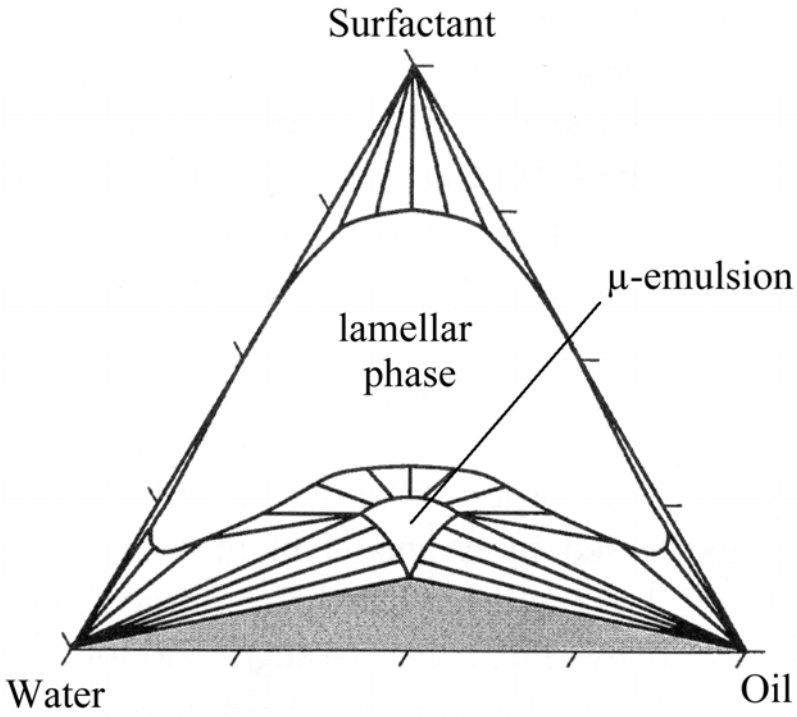


Figure 2-1: Phase behavior of a water-surfactant-oil system. μ-emulsion denotes the microemulsion regions.

Depending on the region of the phase diagram, the nature of the microemulsion changes from oil in water to water in oil through the lamellar phase region. In each region a multitude of microstructure can be observed.

The microemulsion investigated in this work is a microemulsion of styrene in water. Apart from water and styrene, this microemulsion contains sodium dodecyl sulfate (SDS) and 1-pentanol used respectively as surfactant and co-surfactant. The interface between the oil and the water phase is composed mainly of 1-pentanol and SDS, i.e. it is considered to be mainly a monolayer of surfactant and co-surfactant adsorbed at the interface. $^{13}$C-NMR chemical shielding data showed that more than 60% 1-pentanol partitions into the interface[10]. This provides the increased surface area needed for the expanded core and increases the fluidity of the interface to enhance the stability of the microemulsion system. The partitioning of 1-pentanol into the oil phase

increases with increase in the amount of styrene in the system; the mixing of 1-pentanol with styrene lowers the free energy of the solubilized styrene. The fraction of hydrophobic styrene in the interface is small and it increases with increasing styrene in microemulsion. The molar ratio of 1-pentanol to SDS in the interface increases with increasing 1-pentanol/SDS ratio in the emulsion. Based on the partitioning results, the composition of each phase and the size of the microemulsion droplets can be estimated.

For the same amount of 1-pentanol and SDS in the system, the droplet size increases and the droplet number decreases with increasing amount of styrene to maintain a constant interfacial area. The interface area is nearly constant for the same amount of SDS and 1-pentanol used, regardless the amount of styrene. The thickness of the interfacial layer was found to be 1 nm, which is smaller than the 1.66 nm extended length of the dodecyl group. This difference is mainly due to chain protrusion and bending of the SDS molecules in the membrane phase.

The diameter of the microemulsion droplets can be determined according to[40]

$$d = \frac{6 \cdot m_{mon} \cdot M_{surf}}{m_{surf} \cdot A_{surf} \cdot N_A \cdot \rho_{mon}} \qquad 2.1$$

where $M_{surf}$ is the molecular weight of the surfactant, $A_{surf}$ is the specific area of the surfactant molecule, $N_A$ is the Avogadro's number, ρ is the density of monomer (for styrene ρ = 0,910 *g/ml*) and $m_{mon}$ and $m_{surf}$ are the amount of monomer and surfactant used respectively.

This equation can be used when the amount of oil phase is lower compared to that of the water phase. Under this condition, the oil phase is present as little droplets. The sizes of the droplets are in the sub micron range and thus influence the mechanism of particle nucleation when polymerized.

## 2.2. Polymerization in microemulsion

Free-radical polymerization in microemulsion can be carried out with oil or water-soluble initiator. Overall, the steps of microemulsion polymerization are the same as in other polymerization processes i.e: initiation, propagation and termination.

Radical formation:

It is the formation of free radical by the decomposition of initiator.

$$I \xrightarrow{k_d} 2R^{\cdot}$$

Initiation.

This corresponds to the addition of the first monomer unit to the former free radical.

$$R^{\cdot} \xrightarrow{k_i} RM^{\cdot}$$

Propagation.

It is the process of the chain growth.

$$RM^{\cdot} + M \xrightarrow{k_p} RM_2^{\cdot}$$

$$RM_i + M_1 \xrightarrow{k_p} RM_{i+1}^{\cdot}$$

Where $k_p$ is the rate coefficient of propagation of the active center. Usually, it is assumed that $k_p$ does not depend on the chain length.

Termination.

It takes place via two types of bimolecular free radical reactions:

Combination:

$$RM_j^{\cdot} + RM_i^{\cdot} \xrightarrow{k_{tc}} R_{i+j}$$

Disproportionation

$$RM_i^{\cdot} + RM_j^{\cdot} \xrightarrow{k_{td}} RM_i + RM_j$$

The disproportionation occurs with the abstraction of a hydrogen atom from one end to give an unsaturated group and two dead polymer chains.

In contrast to conventional emulsion polymerization, microemulsion polymerization consists of only two types of particles: the monomer-swollen micelles and the monomer swollen polymer particles[10].

The basic studies of the kinetic of microemulsion polymerization used the hypothesis proposed in the emulsion polymerization studies but the mechanism of the polymerization is different. The model system used for these studies was the microemulsion of styrene (oil) in water using water-soluble initiator. In this polymerization, only two intervals are found compared to three in conventional emulsion polymerization. No particle formation is observed in microemulsion polymerization because the reaction takes place inside microemulsion droplets that already exist before the reaction starts. The polymerization rate first increases to a maximum and then decreases[6-8]. The nucleation interval ends when all microemulsion droplets have disappeared, either by becoming polymer particles, or by being consumed by the diffusion of their monomer to polymer particles. The monomer core of the microemulsion droplets disappears early in the polymerization (4% conversion)[10]. What remains are SDS and 1-pentanol and the small amount of styrene in the palisade layer. The newly formed polymer particle grows by recruiting monomer from the microemulsion droplets and the inactive polymer particles, either by diffusion or by collision. The polymerization rate begins to decrease mainly due to the decrease of the monomer concentration in the monomer-swollen polymer particles.

Based on the recent articles published on the investigation of microemulsion polymerization of styrene in water, the essential features are as follows: (1) particle nucleation occurs in monomer-swollen micelles and almost all the radicals in the water phase enter the monomer-swollen micelles and initiate the

polymerization therein (2) with negligible radical termination in the water phase and (3) with negligible radical entry into the performed polymer particle and accordingly (4) all chain stopping events in the active polymer particles are chain-transfer reaction to monomer and (5) the growth of a polymer particle is stopped only by radical desorption from the polymer particle. The average number of radicals per particle is very small (< 0.3) compared to conventional emulsion[6-8, 41, 42].

Polymerization in microemulsion is suitable for the preparation of very high molar mass polymers at rapid reaction rate. This is due to the high monomer concentration within the particles and to the fact that free radicals grow in separate particles preventing their mutual termination.

Polymerizations in inverse microemulsion systems are usually performed by water-soluble monomer[27, 43, 44, 45]. The case of acrylamide has been widely studied by Candau et al[9]. They reported that the rate of polymerization was very high as well as the molecular weight of the product. They also observed a narrow molecular weight and particle size between 20 and 70 nm.

Extensive investigations have been done on the kinetics of microemulsion polymerization using slightly water-soluble monomer like styrene. Guo et al indicated that the nucleation process continues throughout the polymerization[41]. Johnson[42] and collaborators also studied styrene O/W microemulion initiated by both water and oil soluble initiator. Using photocorrelation spectroscopy, they observed a bimodal distribution of particle size. The total conversion was reached in the reaction in less than 30 minutes and the latex obtained were stable and could be diluted. Mamoru and Kiyoshi[6] carried out the microemulsion polymerization of styrene at 50°C using sodium lauryl sulfate and 1-pentanol as emulsifier and co-surfactant, respectively. They observed that both the particle size and the molecular weight of polystyrene remain constant during the course of the polymerization. The same observation was done by Antonietti[7] et al., who pointed out that the particle size could be controlled quantitatively within the

range of 10 to 100 nm by adjusting the weight ratio of emulsifier to monomer initially charged. To achieve this control, high ratio of emulsifier to monomer was used. This high amount of surfactant can cause problems in some applications of the latex obtained. The high value of surfactant to monomer ratio may also be a problem while characterizing the latex obtained from microemulsion polymerization using devices like Transmission Electron Microscopy (TEM) or Atomic Force Microscopy (AFM). Surfactant-free microemlusion has been suggested to clear up this problem but in most cases, it is not a good solution because of a lag on the stabilization of latex particles that may be observed.

Particles size and molecular weight distributions are important parameters for emulsion polymers. Various microscopic processes occurring at the loci of polymerization govern them. A lot of investigations have been done so far to characterize and describe the mechanisms of particle nucleation and growth. It was shown that the polymerizing particles are the loci of the polymerization. Accordingly, fluorescence depolarization will be used online to follow polymerization within these particles. This work focuses on the change of the local viscosity during the process.

## 3. Introduction to Fluorescence

The absorption of photons by a molecule leads to its excitation. An electronically excited molecule can lose its energy by emission of ultraviolet, visible, infrared radiation or by collision with the surrounding matter. Luminescence is thus the emission of photons from excited electronic energy levels of molecules. The energy difference between the initial and the final electronic states is emitted as fluorescence or phosphorescence.

Fluorescence is a spin-allowed radiative transition between two states of the same multiplicity.

$$S_1 \rightarrow S_0$$

Phosphorescence is a spin-forbidden radiative transition between two states of different multiplicity.

$$T_1 \rightarrow S_0$$

Figure 3.1 summarizes photophysical processes involving electronically excited states, mainly, excitation, internal conversion and emission[46,47].

Fluorescence technique is a global name containing specific techniques amongst which: Fluorescence quenching, which depends on the special distribution of excited molecules and quenching species, is a powerful method to study the diffusion of small molecules. Non-radiative energy transfer may be used to characterize a distance within a single macromolecule or distance between constituents of an association complex of macromolecules. The quenching and the energy transfer techniques are used to characterize the dynamics and the structure of systems on the molecular scale. The microenvironment and the local viscosity of the system are better understood by fluorescence depolarization technique in which it is possible to follow the polarization of the emitted light as a function of time after excitation by polarized light.

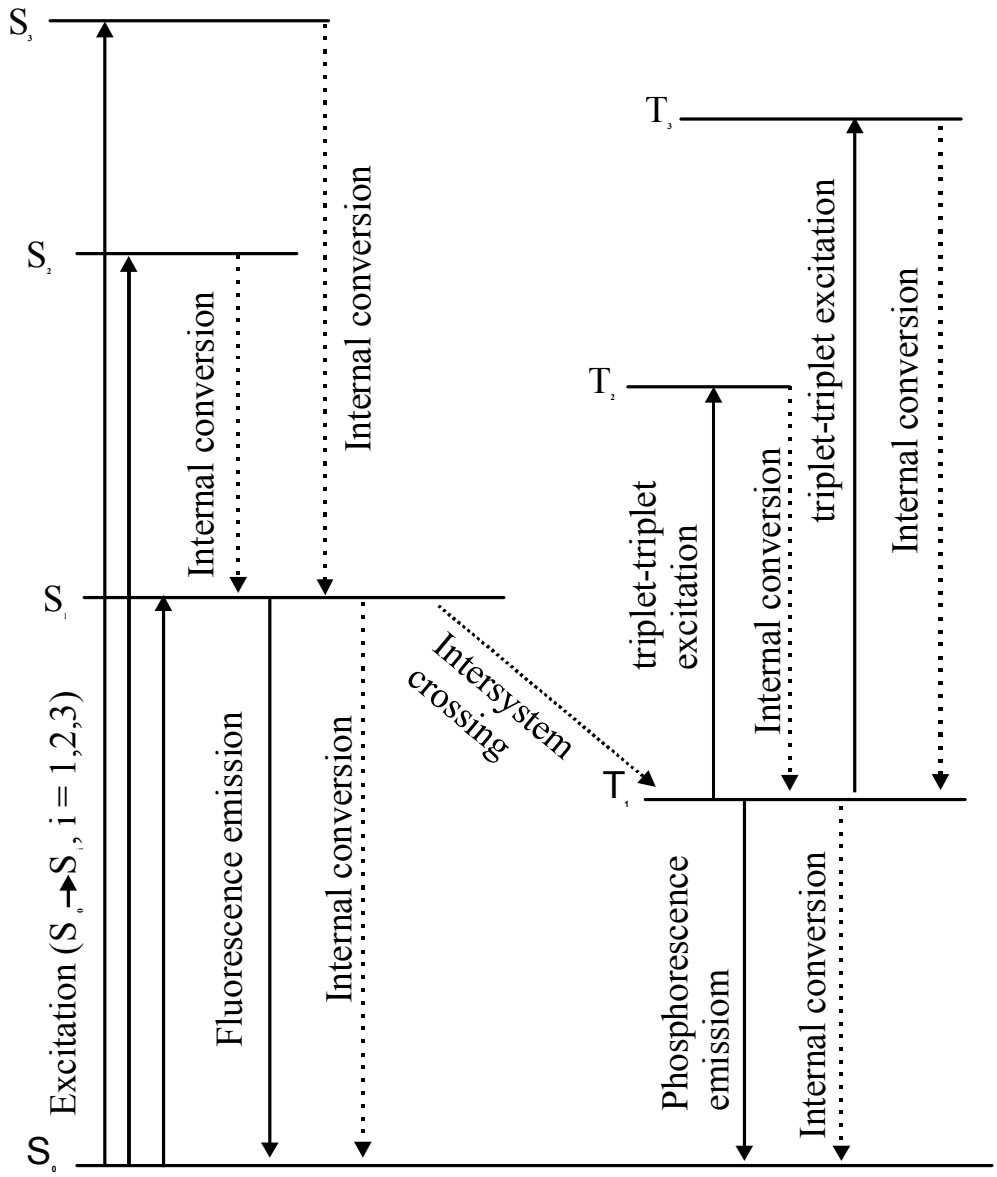


Figure 3-1: A Jablonski diagram showing photophysical processes involving electronically excited states.

### 3.1. Fluorescence spectroscopy

Fluorescence is a radiative emission process occurring from the lowest excited singlet state $S_1$ to the ground state $S_0$. In fluorescence spectroscopy the observed spectra intensity is a function of two variables; the excitation wavelength ($\lambda_{ex}$), and the emission wavelength ($\lambda_{em}$).

The fluorescence property of a compound is conventionally studied by examining both the excitation spectrum and the emission spectrum. The fluorescent spectra are generally plotted with fluorescent intensity *I* (in arbitrary unit) on the ordinate with wavelength (nanometer) of the excitation light or the emission light on the abscissa. Fluorescent intensity can be calculated from the Lambert-Beer law:

$$I_f = I_0\left(1-10^{-\varepsilon c l}\right)\varphi_f \qquad 3.1$$

Where $I_o$ is the excitation radiation intensity in *quanta /s*, $I_f$ is the fluorescence intensity in *quanta/s*, *c* is the concentration of solute in *mol/L*, *l* is the path length of the sample in *cm*, ε is the molar absorptivity (molar extinction coefficient) in *L/mol.cm* and $\varphi_f$ is the quantum yield of fluorescence.

### 3.2 Choice of the fluorescent probe

A fluorescent dye or probe is a molecule, small relative to the investigated system, providing information about the limited volume in which it is found. According to their properties, intrinsic or extrinsic fluorescent probe can be used for the investigation of different media[48,49].

An extrinsic probe is a probe that is freely introduced or covalently attached to the system to be studied. In contrast to the extrinsic probe, intrinsic probe is a naturally occurring molecule or group of molecules, which may contribute to the intrinsic fluorescence of the system.

The choice of the fluorescent probe depends on:

- Stability of the chemical structure
- Place of location in the system to be studied
- Fluorescent efficiency
- Interactions with the system to be studied

Applying fluorescence spectroscopy in natural science has several advantages. These include its high sensitivity which leads to the detection of extremely low concentration of probe; the easy accessibility of nanosecond time scale for dynamics investigations; the great possibility of probe delegation in heterogeneous systems, and its non-destructive characteristics.

### 3.3 Determination of lifetime of fluorescent dye

The fluorescence lifetime of a probe represents the average amount of time the molecule remains in the excited state before its return to the ground state. The lifetime of most of fluorescent probes is in the nanosecond region. It is an essential value in discussing fluorescence depolarization as well as other fluorescence techniques. Studies on the lifetime of the excited state can give significant information about the kinetics of intermolecular reactions such as formation of dimer and excimer[50-52], intermolecular rotational diffusion (Brownian motion), energy transfer and molecular and intermolecular distances[48, 56,57].

The most general and widely used method for time resolved fluorescence studies is time correlated single-photon counting[48]. According to this technique, a pulse of light excites the sample. The relaxation of fluorescent probe from the excited state to the ground state follows the exponential decay law:

$$I_t = I_0 e^{-\frac{t}{\tau}} \qquad 3.2$$

Where $I_0$ and $I_t$ are the intensities at time 0 and $t$ respectively. $t$ is the time at which $I_t$ is measured and $\tau$ is the mean lifetime of the excited single state.

In general, fluorescence decay function can be described by an exponential or sum of exponential described by

$$I_t = \sum_{i=1}^{n} \alpha_i e^{-\frac{t}{\tau_i}} \qquad 3.3$$

In this expression, $\alpha_i$ represents the amplitude of the component at $t = 0$, $\tau_i$ is the decay time and $n$ is the number of decay times[48].

The meaning of the parameters $\alpha$ and $\tau$ depends on the systems being studied. In the case of a mixture of fluorophore, each displaying one of the decay times, $\alpha_i$ depends on the quantum yield, the intensity and the concentration of each fluorophore at the observation wavelength. When a fluorophore is dissolved in a mixture of solvent so that a range of environments exists, then a decay time can be assigned to each of these states. In this case, the pre-exponential values $\alpha_i$ represent the fraction of molecule in each state at $t = 0$. A distribution of decay time is thus expected rather than a limited number of discrete decay times.

# 4. Fluorescence Depolarization

The photoselection of fluorescent probe by polarized light offers the opportunity to study some relevant processes occurring at molecular level in heterogeneous systems. The depolarization of the fluorescence in a polymer system is generally due to Brownian motions of the probe, which occur during the lifetime of excitation. These motions are affected by the physical changes that occur in the immediate environment of the fluorescent probe leading to a change in its polarization[48, 58, 59]. From the depolarization of fluorescence, information such as local viscosity and micromobility[60-62] as well as the micropolarity[63,64] of the system, the relaxation times of polymer[65,66] and local mobility of polymer chain[67-69] can be gained.

## 4.1. Polarized Fluorescence: degree of polarization and anisotropy

A ray of light consists of a magnetic and electric field that are perpendicular to each other and to the direction of propagation of the ray. The electromagnetic field vector has a particular orientation with respect to a given coordinate system, and a beam composed of many rays can be characterized in terms of the overall angular distribution of the electric field vectors. On the two extremes the angular distribution of the ray may be random, resulting in a non-polarized beam, or the rays may be all parallel vectors and be completely polarized[70].

When a sample of randomly oriented fluorescent molecules is exposed to polarized light, preferentially, the molecules having their dipole moment oriented parallel to the direction of the polarized light are selected and excited. If the molecular motion is slow compared to the emission, the emitted light will also be polarized. When the excited molecules rotate rapidly compared to the emission process, the depolarization of the emitted light occurs. The rotational diffusion of the excited molecules is not the only cause of the depolarization, but also a number of phenomena depending on the sample under investigation. The

rate of molecular motion can be estimated by determining the degree of polarization (*P*) or the anisotropy of fluorescence (*r*).

Experimentally, exciting a sample with vertically polarized light and measuring the intensities of vertical and horizontal components of the emitted light determine the degree of polarization *P* or the anisotropy *r*. The anisotropy reveals the average angular displacement of the fluorescent molecule that occurs between absorption and subsequent emission. Figure 4-1 gives the geometrical representation of the system.

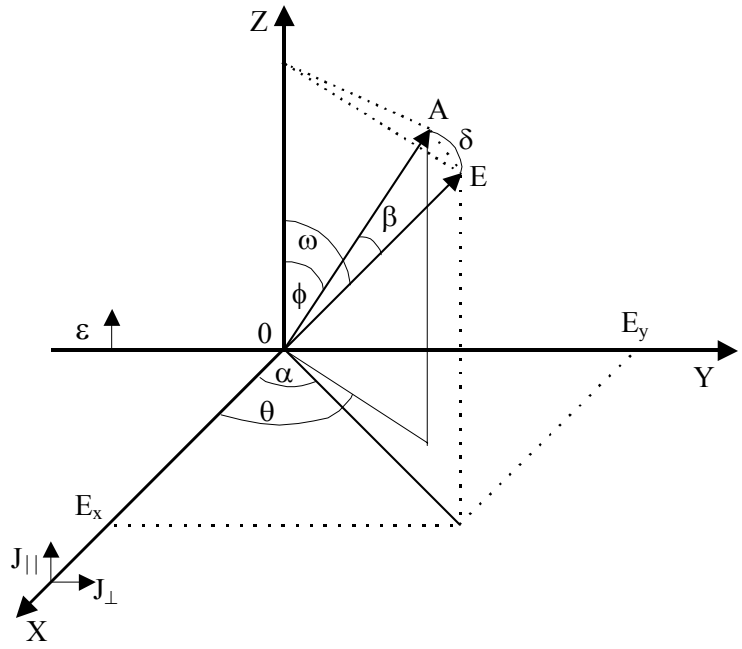


Figure 4-1: Geometry of the system. The incident light is polarized along positive z-axis and the fluorescence is observed along x-axis.

Excitation light ε is polarized in the direction Z. Fluorescence is observed along X; the vectors OA and OE represent the direction of absorption and emission transition moments. δ is the angle between the planes formed by OZA and OZE. α and θ are the angles between the X-axis and the vertical projection of the OA

and OE vectors respectively. ω and ϕ are the angles between the Z-axis and the vectors OE and OA respectively. β is the angle between OA and OE.

The polarization of light emitted by a probe within the irradiated volume may be described in terms of the three components $I_x$, $I_y$, $I_z$ of the intensity along the coordinates x, y, z. The sum of these intensities is proportional to the total radiant energy emitted in all directions:

$$I = I_x + I_y + I_z$$

The exciting beam is polarized along the OZ axis and from the symmetry considerations $I_y = I_x$ and the total intensity is given by:

$$I = I_z + 2I_y \qquad 4.1$$

If the quantities $I_{//}$ and $I_{\perp}$ designate the components of light which are parallel and perpendicular to the electric vector respectively, then $I_z = I_{//}$ and $I_y = I_{\perp}$.

The degree of polarization, $P$, and the anisotropy, $r$, are thus respectively given by equations (4.2) and (4.3).

$$P = \frac{I_{||} - I_{\perp}}{I_{||} + I_{\perp}} \qquad 4.2$$

and

$$r = \frac{I_{||} - I_{\perp}}{I_{||} + 2I_{\perp}} \qquad 4.3$$

The anisotropy and the degree of polarization values can be interchanged using the following equations:

$$P = \frac{3r}{2 + r} \qquad 4.4$$

$$r = \frac{2P}{3 - P} \qquad 4.5$$

The intrinsic value of anisotropy, $r_0$ and the polarization $P_0$ are the value measured when the fluorescent dye remains immobile during the excited state. They are obtained by using a highly viscous solvent or a glass at low temperature in order to avoid Brownian motions. The theoretical values[48] obtainable are as follows:

$-0.2 \leq r_0 \leq 0.4$ for the anisotropy and $-0.33 \leq P \leq 0.5$ for the polarization. The value of $r_0 = -0.2$ is obtained when the excitation and the emission dipole moments are 90° relative to each other.

The theoretical value of the anisotropy $r_0 = 0.4$ is rather difficult to obtain. The major factor responsible for this loss of anisotropy is the displacement of the emission dipole relative to the excitation by an angle θ. This corresponds to a decrease in intrinsic anisotropy by a factor $(3\cos\theta^2 - 1)/2$. The observed anisotropy respectively polarization in a vitrified solution is then a product of the anisotropy due to the photoselection and the loss of anisotropy due to angular displacement of the dipoles.

$$r_0 = \frac{2}{5}\left(\frac{3\cos^2\theta - 1}{2}\right) \qquad 4.6$$

$$P_0 = \frac{3\cos^2\theta - 1}{\cos^2\theta + 3} \qquad 4.7$$

## 4. 2 Rotational diffusion of fluorescent molecules

Rotational diffusion of fluorescent molecules is the principal factor of depolarization of fluorescence in solution[71]. It is thus a key parameter to gain information about the immediate environment of the probe[72]. Therefore, it is important to observe the behavior of the fluorescence anisotropy during the lifetime of the excited state. The rotational diffusion of the probe is characterized by its rotational diffusion coefficient, *R*, and the rotational correlation time ϕ. Using time resolved fluorescence spectroscopy; the relation between these two parameters can be derived.

Following the pulse excitation of the sample, the decay of anisotropy, *r(t)*, for a spherical molecule is a single exponential expressed by

$$r(t) = r_0 \cdot exp\left(\frac{t}{\phi}\right) = r_0 \cdot exp(-6 \cdot R \cdot t) \qquad 4.8$$

It follows that $\phi = (6R)^{-1}$ with $R = kT/6V\eta$.

The rotational correlation time, ϕ, which is a function of the hydrodynamic volume *V* of the rotating species, the local viscosity η, and the temperature of the medium *T*, is given by

$$\phi = \frac{\eta \cdot V_{hydro}}{k \cdot T} \qquad 4.9$$

For non-spherical particles, the rotational diffusion coefficient is a function of the shape of the particles. In this case, the rotational correlation time is obtained by multiplying equation (4.9) by a shape-dependant factor.

$$\phi = \frac{\eta \cdot V_{hydro}}{k \cdot T}\left(\frac{3}{2}\left[\frac{(2-\rho^2)G(\rho)-1}{(1-\rho^4)}\right]\right)^{-1} \qquad 4.10$$

where ρ is the axial ratio (*b/a*), *a* is the length of the major semiaxis, and *b* the length of the minor semiaxis. The factor *G(ρ)* depends on the value of ρ for ellipsoid (prolate ρ < 1 and oblate ρ > 1).

Within this work, the fluorescent probes are assumed to be spherical and also have only one detectable molecular rotation.

The steady-state anisotropy can then be calculated from an average of the anisotropy decay *r(t)* over the intensity decay $I(t)= I_{\parallel}+2I_{\perp}$

$$r = \frac{\int_0^\infty I(t)\cdot r(t)dt}{\int_0^\infty I(t)dt} \qquad 4.11$$

For a single-exponential decay, the equation can be transformed to the following

$$r = \frac{r_0}{1+\tau/\phi} \qquad 4.12$$

Introducing the expression of rotational correlation time ϕ into equation (4.12) leads to

$$\frac{r_0}{r} = 1 + \frac{k \cdot T \cdot \tau}{\eta \cdot V_{hydro}} \qquad 4.13$$

From equation (4.13), known as *Perrin-equation*[72], the viscosity of the immediate environment of the fluorescent molecule is given by

$$\eta = \frac{k \cdot T}{V_{hydro}} \cdot \left( \frac{r_0}{r} - 1 \right)^{-1} \qquad 4.14$$

The hydrodynamic volume of the probe is obtained by measuring the anisotropy of the dye in a homogeneous solution of known viscosities at various temperatures.

The viscosity of the immediate environment of the probe obtained here is different from the viscosity of the whole system. It is known as local viscosity or microviscosity. However, for the system investigated in this thesis, the multiple scattering of the light by particles has to be taken into account.

# 5. Light Scattering

Light scattering has become a standard tool in studying a whole range of materials including gases, pure liquids and solution of both ordinary and, particularly, of macromolecules, colloidal suspensions, glasses and polymers. Its basic principles, which include the theories of electromagnetic radiation and the experimental considerations based essentially on the optic and electronic systems are described in several classical textbooks[73-75].

## 5.1 Size and angle dependence of scattering light

If a molecule is exposed to electromagnetic radiation, i.e. light, it will scatter a part of the incident light due to the interaction of the outer electrons with the radiation. This scattered light depends in character on both the incident light and the molecule itself and so serves as a source of information for either. According to Rayleigh[76] equation, light scattered by particles perpendicular to the primary beam are polarized.

The polarization is often described by a radiation pattern or a polar diagram as shown in figure 5-1[73]. The outer solid line of the figure gives the sum of the two intensities; that is, it gives the angular distribution characteristic of unpolarized light. The vertical component (i.e., the one normal to the plane containing the source, sample, and detector) will produce a vertical oscillating dipole, and this will produce electromagnetic radiation, which will scatter on all directions of the plane with equal intensity. The horizontal component will similarly give rise to an electromagnetic radiation with an intensity distribution in the plane resembling the figure eight (8) so that there will be no scattering at 90°.

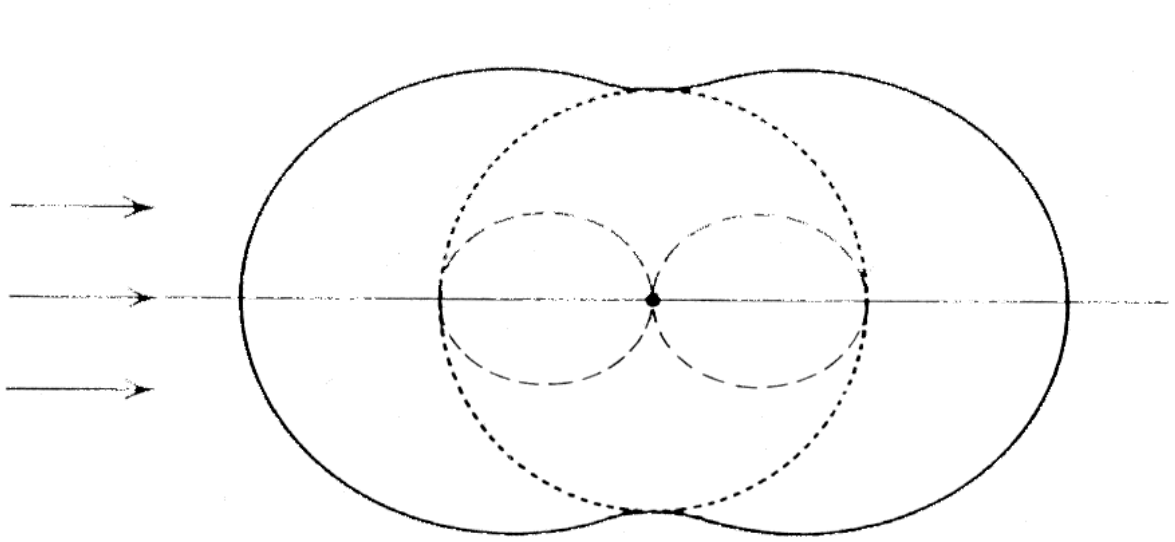

Figure 5-1: Scattered intensities from light polarized in the plane of source, sample, and observer (dashed line) and from light polarized perpendicular to this plane (dotted line).

The anisotropy of the scattering light measured at right angle for polarized or unpolarized incident light should theoretically be 1 as can be obtained in equation 5.1.

$$r = \frac{(I_1 - I_2)}{(I_1 + 2I_2)} = \frac{1 - \cos^2\theta}{1 + 2\cos^2\theta} \qquad 5.1$$

At other angles, the anisotropy of the scattered light will be lower when unpolarized light is used as incident light.

If the particles interacting with the light are large (greater than $\lambda/20$), intra-particle interference causes the polar diagram to become dependent on the particle shape. The polar diagram resulting from the scattered light by large particle is given by figure 5-2[13]. The solid line represents the scattering from sphere whose diameters are approximately one half of the wavelength of the incident light.

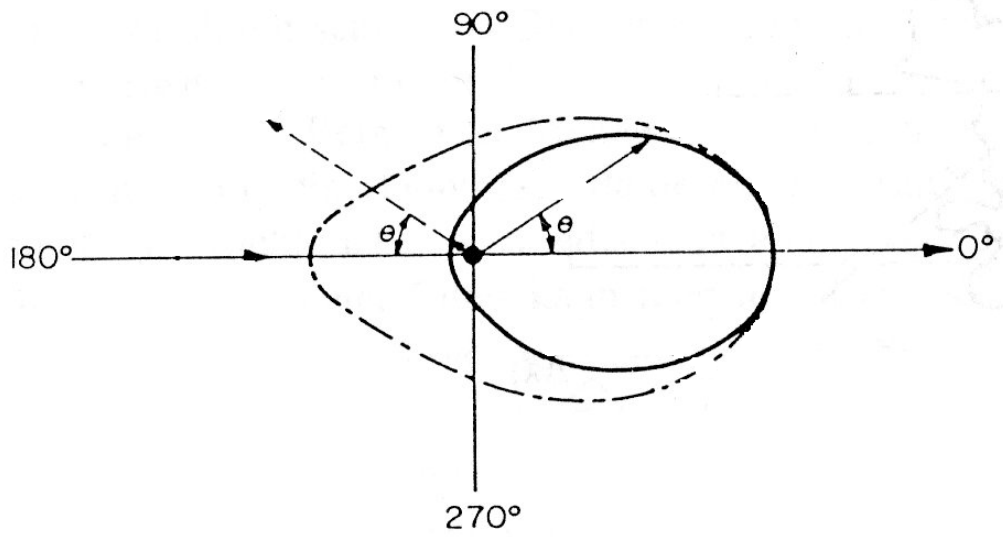


Figure 5-2: Intensity distribution of light scattered at various angles by large particles. The solid line represents the scattering from the particles whose diameters are approximately one half of the wavelength of the incident light.

The intensity of scattering is obtained here while assuming that the particles are small isotropic and diluted. Their separation is so large that in the neighborhoods of any particle the total intensity scattered by all particles is small compared to the intensity of the primary light source. In this system, where it is most probable to have a single scattering, the intensity of scattering light gives information about the size of the scattered particles and the interaction between particles.

The Rayleigh equation leads to the result that light scattered by a particle perpendicular to the primary beam (polarized or unpolarized) will always be completely polarized. This might not be exactly the case and the depolarization may be explained assuming that the particles are not spherical. The fact that the particles are not spherical is not the only factor of the depolarization of scattered

light. Multiple scattering should also be taken into account specially in concentrated solution.

In the case of fluorescence depolarization experiment, multiple scattering is also responsible for some amount of the depolarization in fluorescence light. For this reason, the data related to these intensities of fluorescence and single scattering light from a turbid or concentrated solution have to be corrected.

# 6. Depolarization of fluorescence and light scattering by turbid solution

Among the causes of depolarization of fluorescence in solution, Brownian motions and multiple light scattering are considered to be the most significant. While on the one hand, through the Brownian motion, the anisotropy of fluorescence can be used to gain some information on the system, the multiple scattering, on the other hand makes it difficult to obtain this information.

In fact, when the electromagnetic beam is incident to this medium, photons may be scattered several times before it is detected as illustrated by figure 6-1.

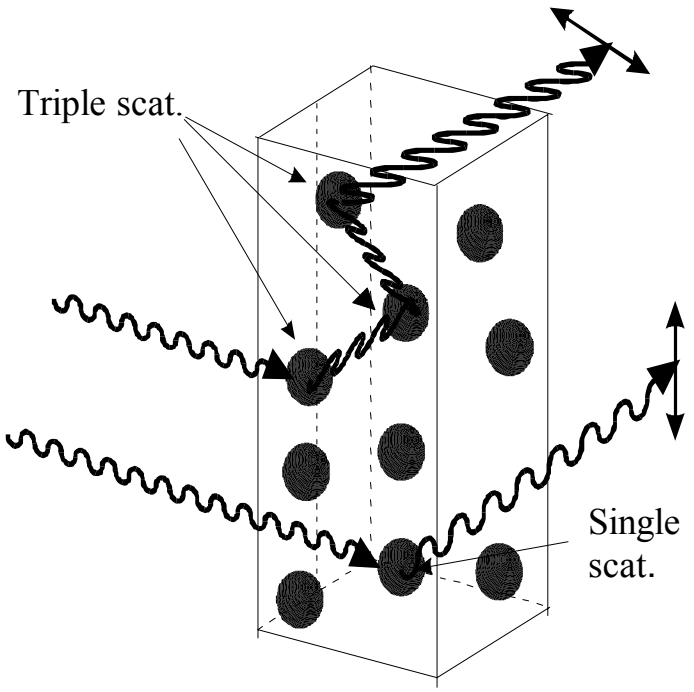


Figure 6-1: Schematic representations of multiple scattering and single scattering inside a cell. Here only triple and single scatterings are illustrated.

This phenomenon called multiple scattering creates a misleading increase in the observed intensity of the scattering and the fluorescence light. Of course, multiple scattering is always present, to some extent, when using an electromagnetic beam in a turbid solution.

Several approaches of correcting multiple scattering effects are being proposed[79,80,81]. Each approach of correction is unique and specific to the system studied. Teale shows in the case of turbid membrane suspension that multiple scattering effects are not negligible as a cause of depolarization of scattering or fluorescence light[82].

The quantity usually extracted from the measurements is the anisotropy of fluorescence. In the presence of multiple scattering, the value of the measured anisotropy is reduced. The theory proposed by Teale[82] to correct the depolarization by membrane suspension is presented here and later on, applied to polymer solution. It is assumed that simple dipole scattering occurs, without depolarization and without internal or external interference. Two cases are considered depending on the scattering position respectively, before and after the fluorescence. The geometry of one scattering process is shown in figure 6-1 for the scattering of excited light, which represents the first case, and in figure 6-2 for scattering of fluorescence for the second case.

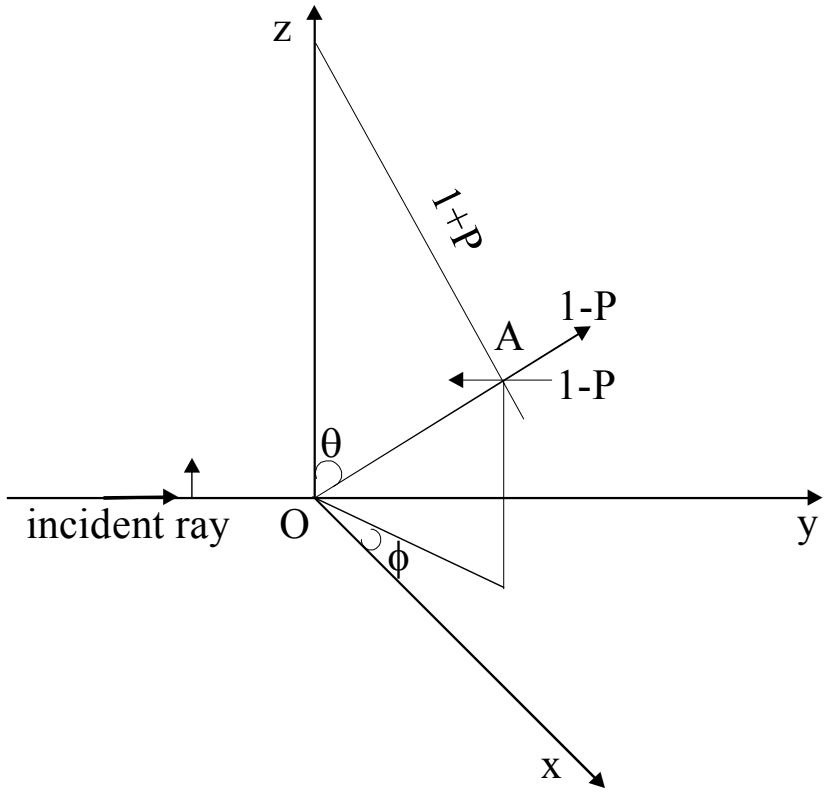


Figure 6-2: Polarized excitation scattered from O and exciting fluorescence at A with polarized *P*. The Intensities of the polarized components are given with respect to the direction OA.

In fig. 6.2 exciting light travels in the Y-direction with the polarization vector along the Z-axis, while observation is made along X-axis. The scattered ray OA, angular-coordinates θ and ϕ, excites fluorescence with polarized *P* and intensities $(1+P)sin^2\theta$ and $(1-P)sin^2\theta$ in the ray direction in the plane of, and normal to the Z-axis respectively. Resolving these intensities in the X-direction, there are components parallel to Z and Y-axes of intensities respectively:

$$I_z = (1+P)sin^2\theta + (1+P)sin^2\theta \cdot cos^2\theta$$

$$I_y = (1+P)sin^2\theta \cdot cos^2\theta \cdot sin^2\phi + (1-P)sin^4\theta \cdot sin^2\phi + (1-P)sin^2\theta \cdot cos^2\phi$$

Integrating these expressions for values of θ, ϕ between 0 and π/2 and combining the results with the polarization *P* of the fluorophore, the observed polarization *P′* is obtained and is given by

$$P' = \frac{\sum I_z - \sum I_y}{\sum I_z + \sum I_y} = \frac{7P}{10 - P} \qquad 6.1$$

Expressing the polarization in terms of emission anisotropy by using equations (3.3) and (3.5) leads to the observed anisotropy of fluorescence.

$$r' = 0.7 \cdot r \qquad 6.2$$

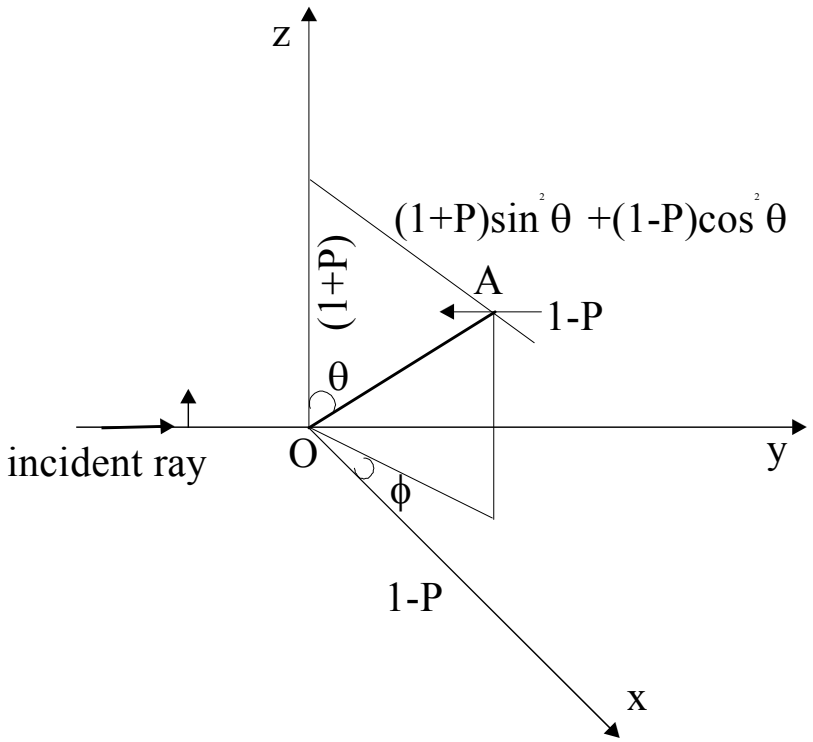


Figure 6-3: Fluorescence with polarized *P* excited by parallel-polarized excitation at O is scattered at A. The Intensities of the polarized components are shown with respect to the x, y and z and to the direction OA.

In figure 6-3 the general emitted ray OA has a component perpendicular to the plane of the Z- axis of intensity $(1-P)$ and a component in the plane of the Z-axis of intensity

$(1+P)sin^4\theta+(1-P)cos^2\theta$ . Resolving along the X-axis gives:

$$I_z=(1+P)sin^4\theta+(1-P)sin^2\theta\cdot cos^2\theta$$

$$I_y=(1-P)cos^2\theta+(1-P)cos^4\theta\cdot sin^2\phi+(1+P)sin^2\theta\cdot cos^2\theta\cdot sin^2\phi$$

Integrating these expression for values of θ, ϕ between 0 and π/2 again leads to:

$$P'=\frac{\sum I_z-\sum I_y}{\sum I_z+\sum I_y}=\frac{7P}{10-P} \qquad 6.3$$

Scattering of fluorescence produces exactly the same depolarization as scattering of exciting light and the observed anisotropy is also given by equation (6.2).

The conclusion drawn here is that each scattering of polarized excitation or emission reduces the resulting anisotropy by a constant factor of 0.7.

If *n* successive scattering processes occur then the observed anisotropy may be expressed as:

$$r_n=0.7^n\cdot r \qquad 6.4$$

where $r_n$ is the anisotropy after n successive scattering processes.

With $n = 0, 1, 2, \ldots, \infty$.

If a dilute scattered solution is used fully polarized light is observed at right angle and $r = 1$. The anisotropy of $n$ successive scattering processes is thus:

$$r' = 0.7^n \qquad 6.5$$

For a set of multiple scattering photons, the anisotropy is obtained by considering an average value of scattering number $\bar{n}$ . The measured anisotropy $r'$ is then given by:

$$\bar{r}' = \frac{\sum_{n=0}^{n=\infty} I_n \cdot r'_n}{\sum_{n=0}^{n=\infty} I_n} \qquad 6.6$$

In this expression $I_n = I_{\|,n} + 2I_{\perp,n}$ and $r'_n$ is the anisotropy measured after $n$ scattering processes.

Combining equations (6.4) and (6.5) leads to the average number of scattering.

$$\bar{n} = ln\left( \frac{\sum_{n=0}^{n=\infty} I_n \cdot 0.7^n}{\sum_{n=0}^{n=\infty} I_n} \right) \cdot ln(0.7)^{-1} \qquad 6.7$$

Teale also found a linear relationship between the absorption $A$ of the scattering medium and the decrease of anisotropy:

$$\frac{r - r'}{r} \approx 2.302 \cdot A \qquad 6.8$$

Following the work of Teale[82], Eisinger and Flores[83] have shown that the fluorescence intensity and polarization as measured in a conventional right angle fluorometer, depends on the absorption and the scattering characteristics of the particles and their concentration in the sample.

Considering a sample with scattering particles and fluorescent probe, whose fluorescence anisotropy is *r*, they were able to determine the observed anisotropy *r´* using vertical polarized light. For this purpose, a dispersion containing a probe in a scattering solution was used. A dilution series of this dispersion was done and during the process, the anisotropy of the probe as a function of concentration of the dispersion was determined.

The semi-logarithmic plot of the observed values of anisotropy *r´* vs. the concentration of the dispersion is a straight line whose intercept gives the true anisotropy of fluorescence *r*.

$$ln\, r' = ln\, r - \gamma \cdot C \qquad 6.9$$

In this equation, $\gamma$ is the anisotropy attenuation coefficient that depends on $\lambda_{ex}$ and $\lambda_{em}$ and on the effective path lengths of the excited and emitted light in the sample cell.

Another method to correct the measured anisotropy was proposed by Tsuneda and co-workers[84]. They used fluorescence depolarization to investigate the mobility of grafted polymer chains. The aim was to obtain the mobility of the chain through the rotational diffusion. Assuming that the optical path length before and after the emission from the probe was almost the same, they showed

that the real value of fluorescence anisotropy caused by rotational diffusion could be calculated using the equation:

$$r = \frac{r'}{(r'_{sc.ex.} \cdot r'_{sc.em})^{0.5}} \qquad 6.10$$

In this expression, $r'_{ex,scat}$ and $r'_{em,scat}$ are, respectively, the values of the anisotropy of scattering at the excitation and emission wavelengths.

Using polymer dispersion, Adams[81] showed the impact of multiple scattering on the single scattering and fluorescence data using a fluorescence depolarization technique and Monte-CARLO-Simulation as well. He was the first to introduce within the above correction equation a κ parameter instead of using 0.5. Good results were obtained depending on the concentration of the dispersion, the position of the fluorescence cell and the wavelength of light. He also established a correlation between the measured anisotropy and the number of scattering processes of an incident photon using a system with changing concentration thus with the turbidity changing with time.

The correction parameter κ shows a clear dependence on the fluorescence anisotropy *r* with the value of – 0.4 (*r* = - 0.1) to 1.9 (*r* = 0.4) as is illustrated in figure 6.3. To describe this dependency, the scattered volume and the change of the direction of polarization of light are to be taken into consideration. The average number of multiple scattering events for fluorescence and scattering light respectively at excitation and emission wavelength is defined. These three parameters are related in equation (6.11).

$$\overline{n}_{Fl.,0} = \frac{\overline{n}_{sc.,ex.,0} + \overline{n}_{sc.,em.,0}}{2} \qquad 6.11$$

A linear relationship is established between the average number of multiple scattering events obtained by computer-simulation and that of the experiment. This relation is given by equation 6.12 in which $D$ is a dimensionless parameter containing the information about the scattered volume, the change of the direction of polarization of light as well as the influence of the intrinsic anisotropy on the change of direction of the polarization.

$$\overline{n} = \overline{n}_0 \cdot D \qquad 6.12$$

$n$ the multiple scattering events calculated is obtained from the anisotropy using equation (6.4.) $n_0$, the actual multiple scattering event is smaller than the measured $n$.

Furthermore, the parameter $D$ can be split into two components: the component $D_p$, which considers the photons scattered from the scattering plan and the component $D_v$ respectively which considers the photons coming out of the scattering volume.

The results of the fluorescence data qualitatively describe the relationship between $D_{Fl,}$ and the anisotropy $r$. This description leads to the relation in equation 6.13.

$$D_{Fl} = \frac{a}{r} \qquad 6.13$$

This equation should only be considered in the case of average number of multiple scattering on a fluorescence light since in the case of pure scattered light the anisotropy $r$ has a value of 1.

Taking into account the equations (6.11), (6.12) and, (6.13) as well as further hypotheses and developments, the dependency of the κ parameter on the measured anisotropy is obtained

$$\kappa = \frac{a_\kappa}{r} + b_\kappa \qquad 6.14$$

The parameters $a_\kappa$ and $b_\kappa$ were determined by a non-liner-least-square-fit.

Figure 6-4 presents the data of an adjustment of the values of κ parameters determined by simulation according to equation (6.14).

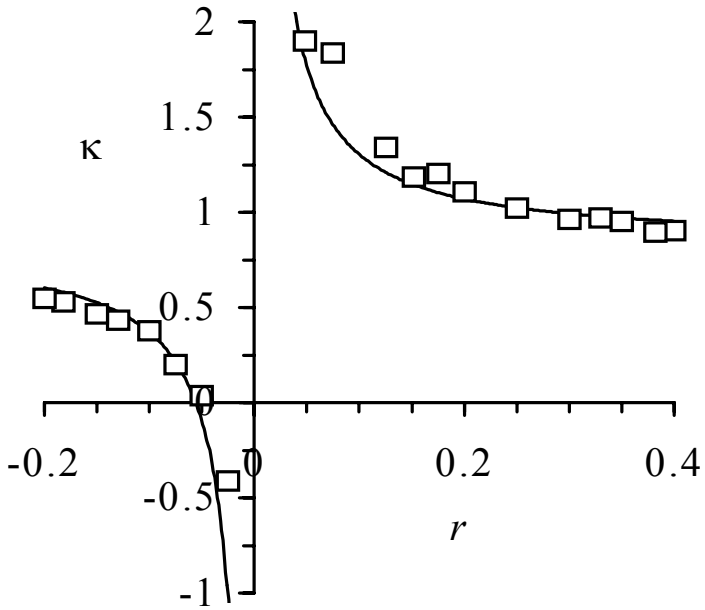


Figure 6-4: Correction parameter κ as a function of the anisotropy *r*. The parameters used for the simulation are 0.047 and 0.83 respectively, for $a_\kappa$ and $b_\kappa$.

It is seen in figure 6-4 that for a value of *r* higher than 0.2, good approximation of κ parameter around 1 is obtained since it changes very little with *r*.

The corrections mentioned above have been applied several times to a specific system with appropriate results. In each case, the results were positive but could not be generalized to other systems. Apart from the studies done by Adams[81], the systems having a turbidity that changes with time have not been investigated enough.

For a better approach of this work, it is necessary to initially describe the system investigated and to determine the photophysical characteristics of the probe.

# 7. Experimental methods

The experimental techniques used for the investigation of the polymerizing microemulsion consist mainly of static fluorescence spectroscopy and time resolve fluorescence spectroscopy.

## 7.1 Description of the system under investigation

### 7.1.1 Preparation of microemulsion

The system under investigation is a microemulsion of styrene in water. The recipe used for the preparation of micro- emulsion was found in literature[41] and consists of: water = 82.25%, styrene = 4.85%, SDS = 9.05%, and 1-pentanol = 3.85%. Styrene has to be purified before it can be used. The purification is performed in order to remove inhibitors and impurities, which can have a detrimental effect on the reaction. Styrene is purified by passing it through a column containing an inhibitor remover from Aldrich® under nitrogen. By this treatment the inhibitors and impurities are adsorbed. The purified styrene monomer was stored in a refrigerator at – 4 °C to prevent thermal auto-initiation of the monomer until it was used. For every microemulsion, a two to five day old monomer was used. 1-pentanol, potassium persulfate, SDS all from Aldrich® were used as received without any further purification. Distilled-deionised water was used in all experiments. The mixture of 1-pentanol and styrene was added to the aqueous solution of SDS under nitrogen. This mixture was then agitated at room temperature for about 10 minutes. The microemulsion obtained was stored in the fridge for 24 hours for equilibrium. After it reached the equilibrium, the microemulsion remained transparent and stable for several months and was ready to be investigated by fluorescence spectroscopy.

For the purposes of the experiment, it was necessary to choose a fluorescent probe and to determine its photophysical properties.

### 7.1.2 Fluorescent Probe

For the investigation, perylene from Aldrich® was chosen as fluorescent molecule. Perylene is hydrophobic and does not interact or destabilize the system as will be shown later. The system is heterogeneous and contains hydrophobic and hydrophilic regions that coexist. During the polymerization, the hydrophobic region consists mainly of micelles and polymer particles. The probability that the probe remains in surfactant assembly and/or in interface between water and polymer particles exists. In this study, perylene is assumed to be inside the micelles as far as it was mixed to the monomer before the polymerization. This assumption appears to be the most probable if one takes into account the fact that perylene is hydrophobic. Perylene was chosen also because of its rigid structure that avoids depolarization due to the rotation of side structure. It also has a high and constant value of intrinsic anisotropy of excitation, $r_{ex}$, and emission $r_{em}$ at about 0.33 (fig. 7-1). The lifetime of the excited state of perylene is short enough to avoid depolarization due to the rotation of the constrained medium, i.e. the polymerized microemulsion particles.

From the excitation and emission spectra of perylene (fig. 7-1), it is observed that both spectra have limited overlap and their second maxima are sufficiently separated. These second maxima are the ones used during static fluorescence measurements.

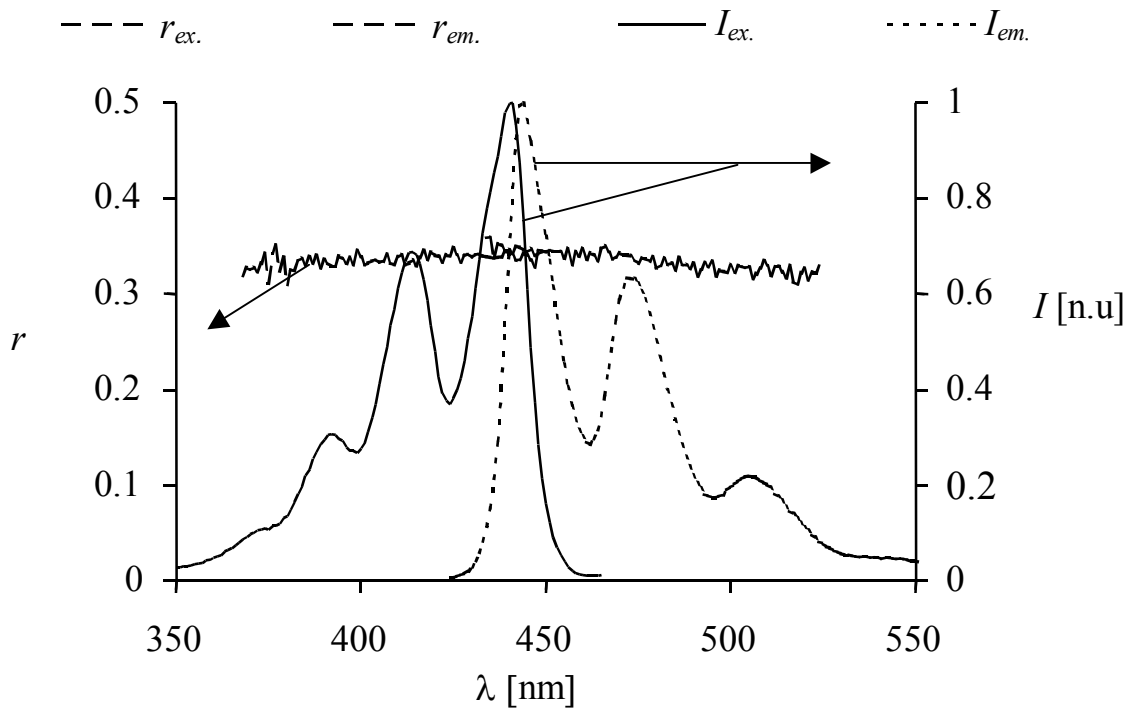


Figure 7-1: Excitation ($I_{ex}$) and emission ($I_{em}$) spectra of perylene measured at $\lambda_{ex}$ = 415 nm and $\lambda_{em}$ = 474 nm and anisotropy of excitation ($r_{ex}$) and emission ($r_{em}$) obtained in glycerol at –5 °C.

In glycerol at –5°C, perylene is considered to be immobile. The anisotropy $r_0$ calculated here has a value of 0.33 and is called intrinsic anisotropy (fig. 7-1). It is very close to the theoretical value of $r_0$ = 0.4 that could be obtained. From this plot it can easily be observed that the anisotropy of emission $r_{em}$ and that of excitation $r_{ex}$ have a constant value which is very important for the purpose of this work.

The photophysical properties and the structure of perylene are shown in figure 7-2.

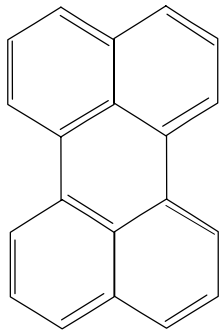

Hydrodynamic radius: 0.22 nm

Lifetime in glycerol: 4.3 - 4.6 ns

$\lambda_{ex} = 415$

$\lambda_{em} = 474$

$r_0 = 0.33$

Figure 7-2: Photophysical properties and structure of perylene.

The intrinsic anisotropy $r_0$ and the hydrodynamic volume of perylene were determined in glycerol at a low temperature (0°C). Solution of $10^{-4}$ mol/L was prepared with Toluene. One ml of this solution was introduced in a 10 ml volumetric flask and evaporated with clean nitrogen. The solute was dissolved in few drops of acetone. The volumetric flask was then filled with 10 ml glycerol under nitrogen. The sample was then shaken at room temperature and stored at $40^{o}$ C for equilibrium. The sample, having a concentration of $10^{-5}$ mol/l, was then ready to be used.

Table 7-1 Variation of glycerol at viscosity with varying temperatures[85, 86].

| T[°C] | -10 | 0 | 10 | 20 | 30 | 40 | 50 | 60 | 70 | 80 |
|---|---|---|---|---|---|---|---|---|---|---|
| η[cP] | 41.32 | 12.03 | 3.90 | 1.40 | 0.56 | 0.25 | 0.12 | 0.07 | 0.04 | 0.03 |

The anisotropy *r* of perylene at these temperatures was calculated. From these data, the plot shown in figure 7-3 was realized. This plot depicts a decrease in anisotropy with temperature as expected.

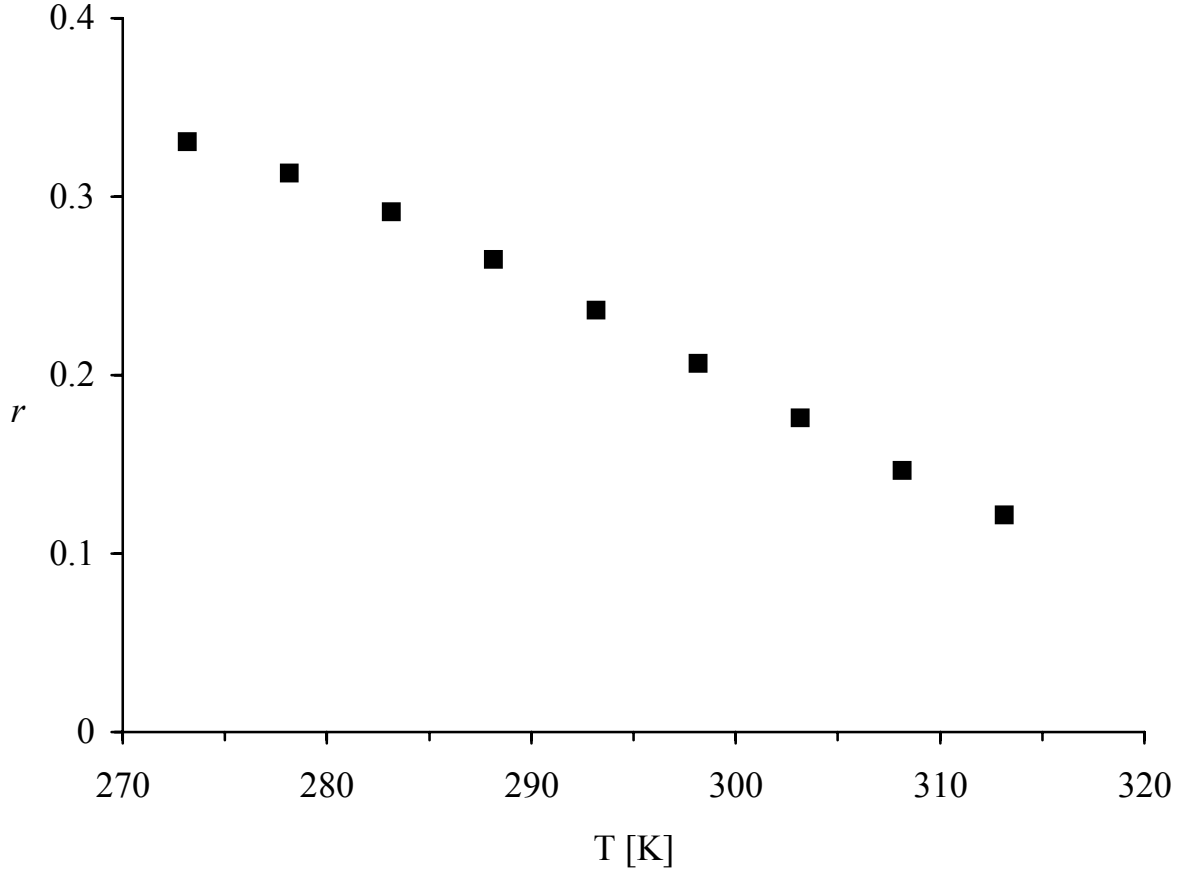


Figure 7.3: Fluorescence anisotropy *r* of perylene in glycerol as a function of temperature.

Figure 7-4 presents the data of the viscosity of glycerol calculated by fluorescence depolarization as a function of temperature. These data are fitted with the value found in literature. A good correlation between the calculated viscosity and those obtained from the literature was observed. This indicates that

the fluorescence depolarization technique applied to perylene, can be used to determine the viscosity in a homogeneous fluid.

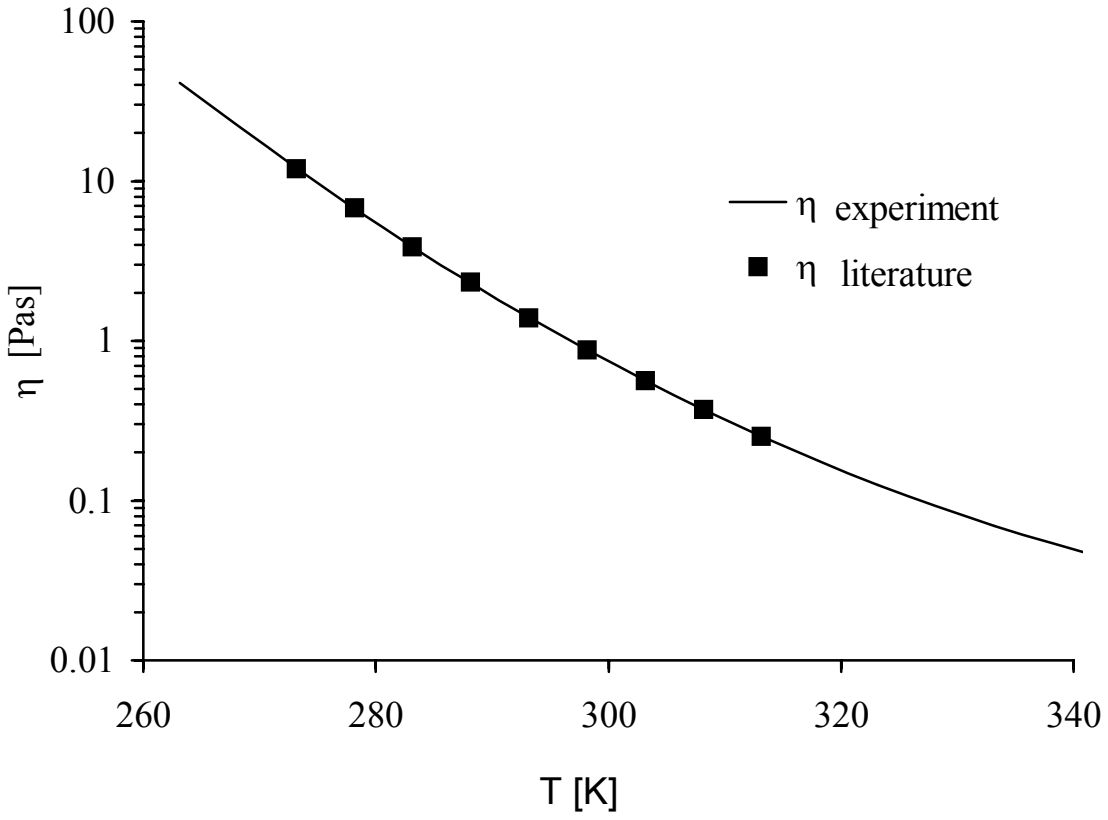


Figure 7-4: Viscosity $\eta$ of glycerol as a function of T. the square (■) are obtained by fluorescence depolarization and the line (—) is the fit with data from literature.

### 7.2 Polymerization procedure

Fluorescence cell with a volume of 4 mL was filled with microemulsion containing perylene under nitrogen. The amount of initiator needed (between 0.3 and 0.5 mM) was added to the system. The microemulsion was polymerized by thermal degradation of water-soluble potassium persulfate (KPS) at 50$^{o}$ C.

During the polymerization, the microemulsion became slightly turbid and the dispersion obtained at the end of the polymerization was bluish.

The monomer conversion was determined by dilatometry using a homemade dilatometer. This dilatometer was built up using a 0.1 ml pipette as capillary and a quadratic fluorescence cell from HELLMA®. These cells are sealed with special screw caps. These special caps, made mainly of Teflon and PVC were built in laboratory. The pipette was fitted into the Teflon and put in top of the fluorescence cell. A PVC tail was used to attach the Teflon containing pipette to the quadratic fluorescence cell.

In a different series of polymerization, the conversion was followed by gas chromatography. These experiments were done at the TU Eindhoven in the group of Prof. Dr. A. Herk. The European Graduate School (EGS) on the „Microstructural Control In Free-Radical Polymerization“ supported the material and the stay in Eindhoven. A sample was collected during the polymerization and quenched with hydroquinone.

Gel Permeation Chromatography (GPC) was used to measure the molecular weight of polymer produced. Transmission Electron Microscopy (TEM) and Atomic Force Microscopy (AFM) were used to determine the shape of particles. Dynamic light scattering, TEM and AFM were used to determine the size of the particles. The dynamic light scattering and the Transmission Electron Microscopy experiments were also done in TU Eindhoven.

## 7.3 Fluorescence methods

### 7.3.1 Time-resolved fluorescence spectroscopy

The fluorescence decay of the probe was measured using time-correlated single-photon counting. The spectrometer was equipped with the nF900 flashlamp from Edingburgh Instruments able to produce nanosecond and sub-nanosecond

light pulses with repetition rates up to 40kHz. This apparatus allows the determination of the lifetime of fluorescent probe.

A special sample holder linked to a thermostat was used, making it possible to follow the polymerization while measuring the decay of the fluorescence probe. Before every experiment, the profile of the lamp was measured using a turbid plate without filter. During the reaction, fluorescent photons were collected in intervals of 30 seconds each.

An in house program written by J. Adams was used to analyze the data of the fluorescence decay. It came out that the decay of the fluorescence intensity follows a mono-exponential decay given by:

$$I = Ae^{-\frac{t}{\tau}} \qquad 7.1$$

The least square fitting analysis is used to determine the lifetime and the pre-exponential factors.

This method, which is quite common, uses an iterative reconvolution process.

It takes into account the instrument response function $L(t_k)$, which is collected by using a dilute scattering solution and no emission filter, the measured data $N(t_k)$, and the calculated decay $Nc(t_k)$. The calculated decay $Nc(t_k)$ that is called the fitted function represents the convolution of $N(t_k)$ and $L(t_k)$. These functions are in terms of discrete time $(t_k)$ because the counted photons are collected into channels, each with a known time $(t_k)$ and a width $\Delta t$.

The concept of convolution states that each excitation function is assumed to induce an impulse response at $t_k$.

$$I(t_k) = L(t_k) \cdot I(t - t_k)\Delta t \qquad 7.2$$

with $t > t_k$

The measured decay is the sum of the impulse response created by all the individual function excitation pulses occurring until $t_k$.

$$N(t_k) = \sum_{t=0}^{t=t_k} L(t_k) \cdot I(t - t_k)\Delta t \qquad 7.3$$

For small value of $\Delta t$, the measured decay is expressed in terms of convolution integral given by

$$N(t_k) = \int_{0}^{t} L(t_k) \cdot I(t - t_k)dt \qquad 7.4$$

With the Least Squares Analysis Method, it is possible to obtain the parameter values which provide the best match between the data $N(t_k)$ and the calculated decay using assumed parameter values. This is accomplished by minimizing the quality of the fit parameter $\chi^2$.

$$\chi^2 = \sum_{k=1}^{n} \frac{1}{\sigma_k^2} [N(t_k) - N_c(t_k)]^2 \qquad 7.5$$

From the Poisson statistic of the fluorescence emission, the standard deviation, $\sigma_k$, is known as: $\sigma^2_k = N(t_k)$; equation (7.5) is thus transformed into:

$$\chi^2 = \sum_{k=1}^{n} \frac{[N(t_k) - N_c(t_k)]^2}{N(t_k)} \qquad 7.6$$

This procedure of matching the calculated curves to the measured data is frequently referred to as deconvolution[48], which is inaccurate. In reality, an assumed decay law $I(t)$ is convoluted with $L(t_k)$, and the results are compared with $N(t_k)$. This procedure is more correctly called iterative reconvolution[48].

It was possible during the experiment to record the overall conversion of monomer to polymer using our homemade dilatometer and simultaneously measure the change in lifetime of the excited state.

### 7.3.2 Polarized fluorescence spectroscopy

During the polymerization, static and polarized fluorescence spectra as well as polarized fluorescence and scattering data were recorded. The fluorescence spectrometer used for these purposes is a Spex Fluorolog2® equipped with a single-photon counting unit from EG&G Ortec®. The source of light is a high pressure Xenon arc lamp (Osram, type XBO, 450 watt). The selection of the wavelength was done by two double grating monochromators (type Spex 1680) with a grating of 1200 line/nm and a blaze wavelength of 250 nm for the excitation monochromator and 500nm for emission monochromator. The rotating polarizers used, respectively, for excitation and emission were Glan Taylor and Glan Thomsom from Hanle®. The sample chamber with an angle of $90^{o}$ between excitation and emission light beam was provided with a positioning desk allowing it to optimize the position of the quadratic cell in the light path. The slits of the double grating monochromator were at about 5.4 nm during the experiment. To record the emission intensity, the excitation wavelength was maintained constant at 415 nm while the emission wavelength varied from 350nm to 600 nm with an interval of $\Delta\lambda$ = 1nm.

For every measurement, a quantum correction curve of the optical components sensitivity was determined using a solution of Rhodamin B in ethylene glycol ($c$ = 4g/l), for the excitation and emission spectra. For the details of this procedure see reference 48. The corrected spectra are obtained by multiplying the measured intensity by the quantum correction curve and the inverse of the reference intensity.

From these measurements, the anisotropy of fluorescence was determined as:

$$r = \frac{I_{VV} - I_{VH} \cdot G_l}{I_{VV} + 2 \cdot I_{VH} \cdot G_l} \qquad 7.7$$

with $$G_l = \frac{I_{HV}}{I_{HH}}$$

$G_1$ is the correction factor having a value between 0.9 and 1.1. This correction factor $G_1$, used to correct the sensitivity of the optics components for different polarized light, is measured for every experiment.

The total intensity measured by the polarized light was given by: the denominator of equation (7.2) that is, $I = I_{VV} + 2\, I_{HV}\, G_1$.

During the scattering measurement, the two monochromators were set at the same wavelength and the intensity of light scattering observed was about 4 orders of magnitude higher compared to that of fluorescence. Interposing a neutral filter between the sample and the detector reduced the intensity of scattering light. This neutral filter has no influence on the polarization of the spectrometer and reduces the scattering intensity by a factor of about 200, whereby it was assumed that the photomultiplier working in the photon counting mode could individually detect all photons hitting the cathode.

A computer-controlled thermostat also monitored the temperature inside the sample holder during the experiment.

To observe the behavior of multiple scattering as a function of concentration of the polymer dispersion on the fluorescence anisotropy and single scattering as well, a dilution series of polymer dispersion was done.

During the experiment, the wavelengths of excitation and emission light were set constant at their maximal values. Initially, 2 ml of bi-distilled water was put inside the cell of 4.5ml volume and then the dispersion was continuously added. A computer-controlled pipette Edos 5221 from Eppendorf-Netheler-Hinz® was used for the automatic control of the amount of latex added. The system was set

in such a way that between the change of the concentration and the next measurement, the mixture was stirred for 30 seconds. The description and more information on the setup can be found elsewhere[87]. A total volume of 1.25 ml latex was automatically added into the cell by fraction as follows: 25 times 10µl, 20 times 20µl, and 15 times 40µl.

## 7.4 Characterizations of the latex

### 7.4.1 Conversion

Conversion was measured by two techniques, namely, dilatometer and GC (gas chromatography).

Dilatometer utilizes the volume change that occurs upon polymerization to follow conversion versus time. This cell was placed in a special sample holder related to a thermostat by isolated rubber tubes. As the desired temperature is reached in the thermostat, valves were opened and the hot water heated the sample. After the heating period, the temperature remained constant and the volume change of the polymerizing system is quantitatively related to the percentage conversion. The movement of the meniscus during the processes is mainly due to two factors:

1. thermal expansion of the solution within the heating period.

2. the isothermal contraction due to polymerization.

An example is shown in figure 7-6. After 15 minutes, the effects due to thermal expansion become negligible and the volume remains constant for 2 or 3 minutes and the polymerization starts. As the polymerization starts, a contraction of volume occurs due to the fact that the density of the form polymer is higher than that of the monomer. This behavior can well be observed on the plot of the height of solution in the capillary versus reaction time. In this

experiment the time $t = 0$ corresponds to the moment at which the valves of the thermostat are opened and the water at the desired temperature starts to flow through the sample holder.

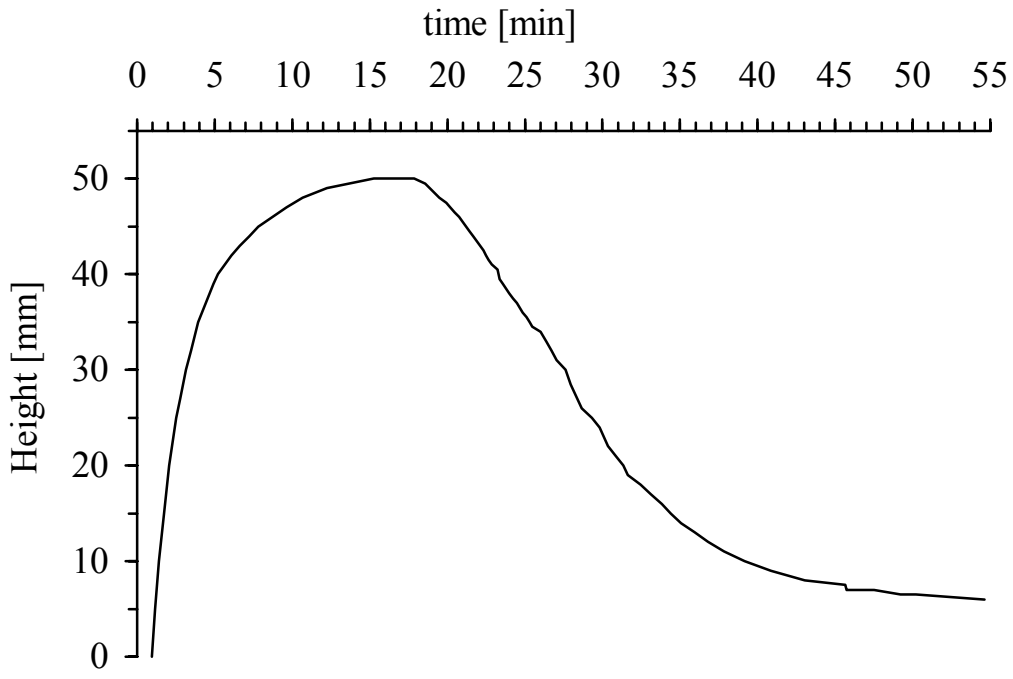


Figure 7-6: plot of the evolution of the height of the solution inside the capillary during the reaction.

At the same initial conditions for different polymerizations, the plot of the height as a function of time appears different up to the maximum value of the height. The difference is mainly observed in the time axis where the thermal equilibrium leading to a plateau at this maximum is more pronounced. It is important to mention that the plot of conversion versus time obtained behaves in the same way after the maximum position is reached. Due to the difference in the duration of the equilibrium period (2 to 4 minutes), the conversions start at different period for different experiment.

It can readily be shown that there is a linear relationship between the degree of conversion in a polymerizing system and the change of the height of solution

inside the capillary. This linear relationship provides that the monomer and polymer mix without change in volume. The volume change on polymerization can be assumed to be a constant increment for each monomer used up.

Assuming $v_t$ the volume of the polymer/monomer mixed phase at conversion time $t$ and $v_0$ the volume of the monomer at time $t = 0$, the volume of the reacting system is given by:

$$v_t = v_0 + \Delta v_t \qquad 7.8$$

where $\Delta v_t$ is the change of volume at time $t$.

At $t = \infty$, the final volume change is obtained from the equation 7.8 and is given by:

$$\Delta v_\infty = v_0 - v_\infty \qquad 7.9$$

Equations (7.8) and (7.9) can be divided by the section $s$ of the capillary to obtain the change of height at time $t$ and at $t = \infty$ respectively. The volume change at time $t$ normalizes by that at $t = \infty$ gives the final volume change at $t = \infty$ and gives access to the conversion deduced from the change of height.

$$\frac{\Delta v_t}{\Delta v_\infty} = \frac{v_0 - v_t}{v_0 - v_\infty} \cdot \frac{s}{s} = \frac{h_0 - h_t}{h_0 - h_\infty} \qquad 7.10$$

Equation (7.10) gives the relative conversion measured in the volume reference frame, which can be considered in mass reference frame immediately. The conversion between 0 and 1 is clearly expressed by:

$$U_t = \frac{h_0 - h_t}{h_0 - h_\infty} \qquad 7.11$$

The conversion obtained by dilatometer was deduced directly from the change of the height inside the capillary (here a 0.1ml pipette). No calibration was done to obtain these curves.

A HP5890 gas chromatograph from the group of Pr. Dr. A. *van* Herk at the Technical University of Eindhoven was used to determine the conversion and the amount of residual monomer. It was equipped with an auto-sampler and Alltech AT-wax column (length 30m, film thickness 1,0µm). The polymerization was performed in a nitrogen atmosphere while maintaining mild nitrogen flow (< 2ml/min) at 50°C. Offline samples were diluted in tetrahydrofurane (THF) and analysed by GC. 1-pentanol was used as internal standard in the GC analysis.

The conversion is obtained from the area of the peak representing variation of the internal standard and the monomer during the polymerization. If $A_p$ is the area of the peak devoted to 1-pentanol and $A_m$ that of the monomer, the amount of polymer at each time $C_t$ will be given by:

$$C_{t,GC} = \frac{\left(\frac{A_p}{A_m}\right)_t - \left(\frac{A_p}{A_m}\right)_0}{\left(\frac{A_p}{A_m}\right)_t} \qquad 7.12$$

### 7.4.2 Particles size and shape

The particle size of the latex was determined by Photocorrelation Spectroscopy (PCS) using a Malvern light scattering spectrophotometer from the group of Prof. *van* Herk of the Technical University of Eindhoven. The measurements were performed at room temperature using a cylindrical glass cell filled with the sample and sealed with glass stopper. Prior to the measurement, the latex sample was diluted with bi-distilled water until the volume fractions of the particles

were in the range 0.01 – 0.1. An average hydrodynamic radius of the latex particles ($R_h$) was calculated from the intrinsic diffusion coefficient ($D_0$).

Using PCS, it was in this case impossible to determine the size of the microemulsion. In literature[17,32] the sizes of microemulsion droplets are reported to lie between 5 and 15 nm. Taken the specific surface area[88] of SDS $A$ = 0.56 $nm^2$ and using equation 2.1 of page 5, the size of the microemulsion was calculated. A diameter of about 3 nm was obtained which is close to 5 nm that could be expected.

The size and the morphologies of the polystyrene micro sphere particles were also investigated using TEM and AFM. Before TEM and AFM measurements, dialysis of the latex was done during a period of five weeks to remove the remaining monomer and surfactants.

# 8. Results and discussion

## 8.1 Process of polymerization

Polymerization in microemulsion produces ultrafine polymer particles. At the end of the process, the microemulsion polymers are stable, bluish and less translucent than the original microemulsion. The turbidity of the system increases as the polymerization advances. The process can be more understood by looking at the rate of the polymerization.

### 8.1.1 Polymerization Rate

Figure 8-1 shows an example of the monomer conversion versus time curves for the microemulsion system studied. The similar behavior of the two plots is a proof that during the thermal expansion observed when using a dilatometer, no significant polymerization occurs and that the homemade dilatometer is good enough to be used.

These plots of conversion versus time can be divided into three distinct reaction regions whereas the rate-conversion plot (in inset) shows only two regions.

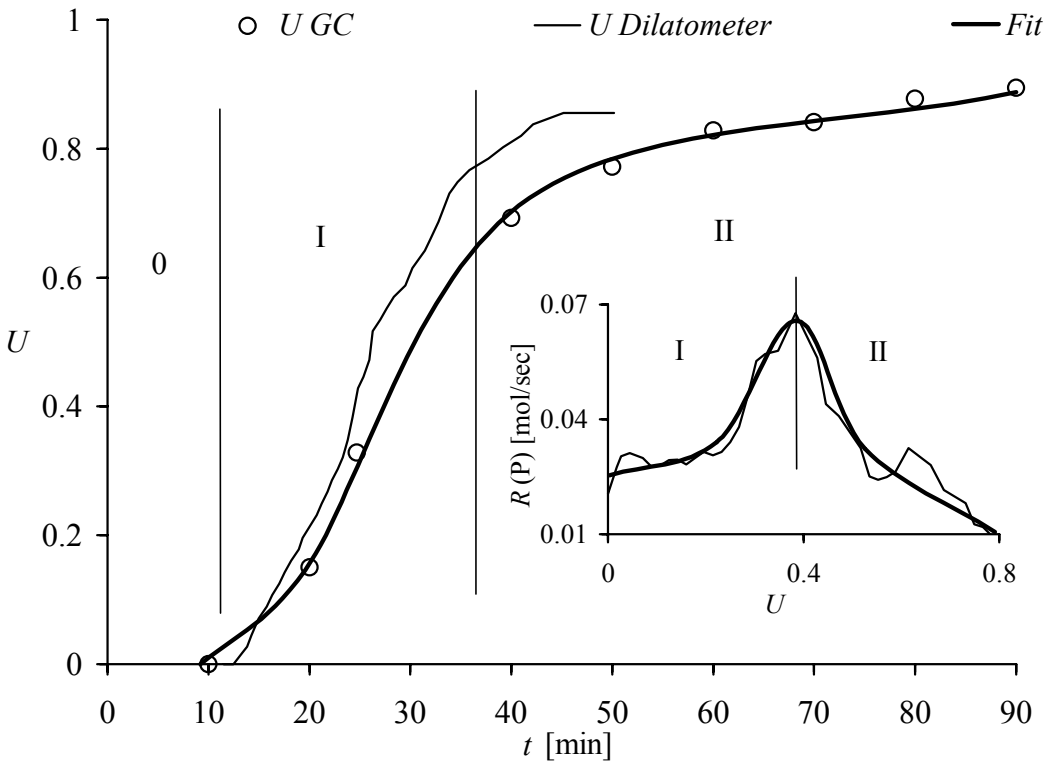


Figure 8-1: Monomer conversion (*U*) versus time curves obtained by dilatometer (•) and conversion obtained by gas chromatography (•) and its fit curve (——). Inset: Plot of the rate of the polymerization versus conversion and the fit curve.

The first region, denoted 0 in the figure 8-1, on the conversion-time plot is the induction period of the polymerization. It varies from 0 to 15 minutes depending on the individual experiment. The duration of this period results in the combined effect of three factors namely: the heating, the inhibition and the thermal equilibrium. The thermal equilibrium lasts for about 2 to 4 minutes as can be seen in figure 7-6 and occurs just before the polymerization starts. During the inhibition period, residual oxygen and other impurities capturing radicals inhibit the polymerization. This conclusion is confirmed by the similarity between the conversion measured by dilatometer and that measured by gas chromatography. Usually, the induction period is not mentioned in the microemulsion process and only the two regions known as interval I and interval II are considered. These regions correspond to those found in the rate-conversion plot.

The second region is characterized by an increase in the rate of polymerization with conversion. This region, known as interval I in mechanisms of microemulsion polymerization[41], corresponds to the creation of new polymerization loci in the existing microemulsion droplets. The increase in the rate of polymerization in interval I is due to the increasing number of polymerization loci with time. At the end of interval I, all the microemulsion droplets disappear either by becoming polymer particles or by being consumed through diffusion of monomer from the droplets to polymer particles.

At conversion around 30 %, interval I ends and the rate of polymerization starts to decrease marking the beginning of interval II that is considered here to be the third region of the conversion time plot. This decrease in rate is mainly due to the decrease in monomer concentration inside the monomer-swollen polymer particles.

### 8.1.2 Particle Size Distribution and particle shape

The average particle size and the particle distribution are important parameters for the quality and the applications of the latex. These parameters were determined by dynamics light scattering by taking offline samples during the polymerizing process. The particle shape and the average particle diameter were determined by AFM. Figure 8-2 shows the diameter of the particles plot as a function of the conversion of monomer to polymer during the reaction.

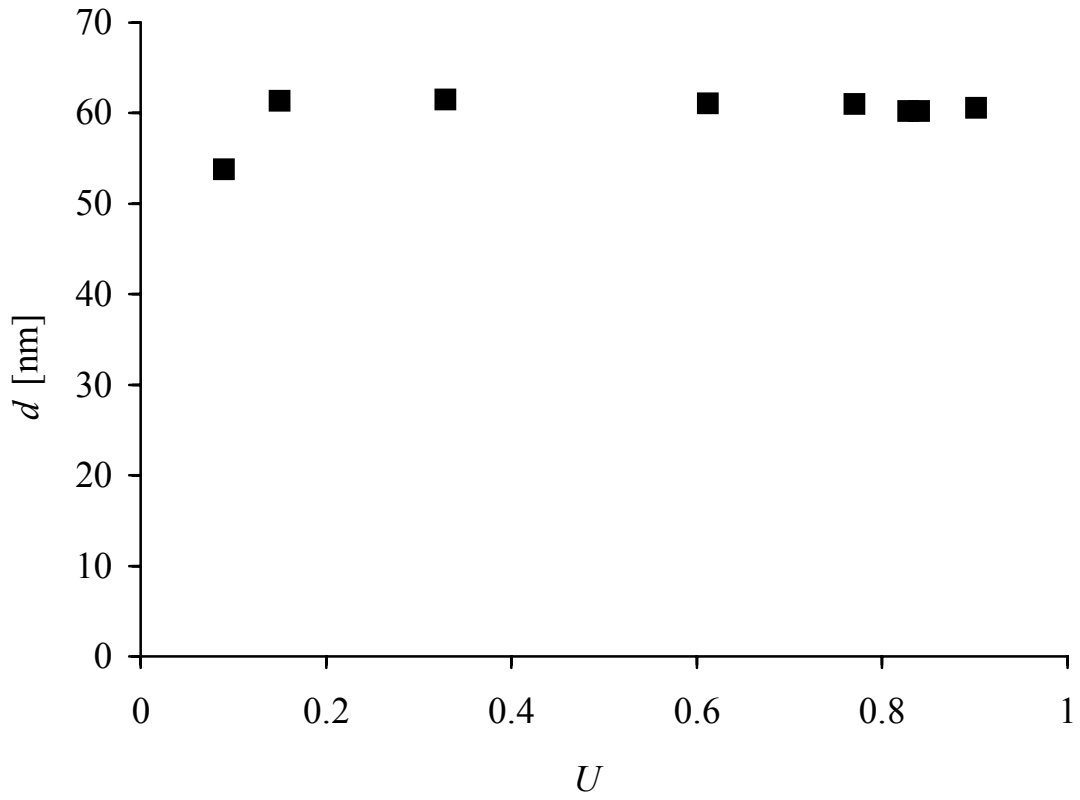


Figure 8-2: Change of particle size (■) as a function of monomer conversion during the polymerization. Data from light scattering

Using the assertion from the literature[17,32] that the size of the microemulsion lies between 5 and 15 nm and considering the plot of the size of the particle versus conversion (figure 8-2), it is seen that a tremendous increase in the size of the particle is observed between 0 and 10% conversion. Around 20 % conversion, an average maximum diameter of ~ 65 nm is reached.

Figure 8-3 shows examples of particle distribution measured at three different times by light scattering during the polymerization. The polydispersity does not vary strongly and has the value of 1.3 in average. This leads to the conclusion that the particle size distributions obtained are narrow. The percentage of particles having the same size is nearly constant at each stage of the

polymerization. For this reason, the global size of the particle does not really change with the conversion during the process (fig. 8.2).

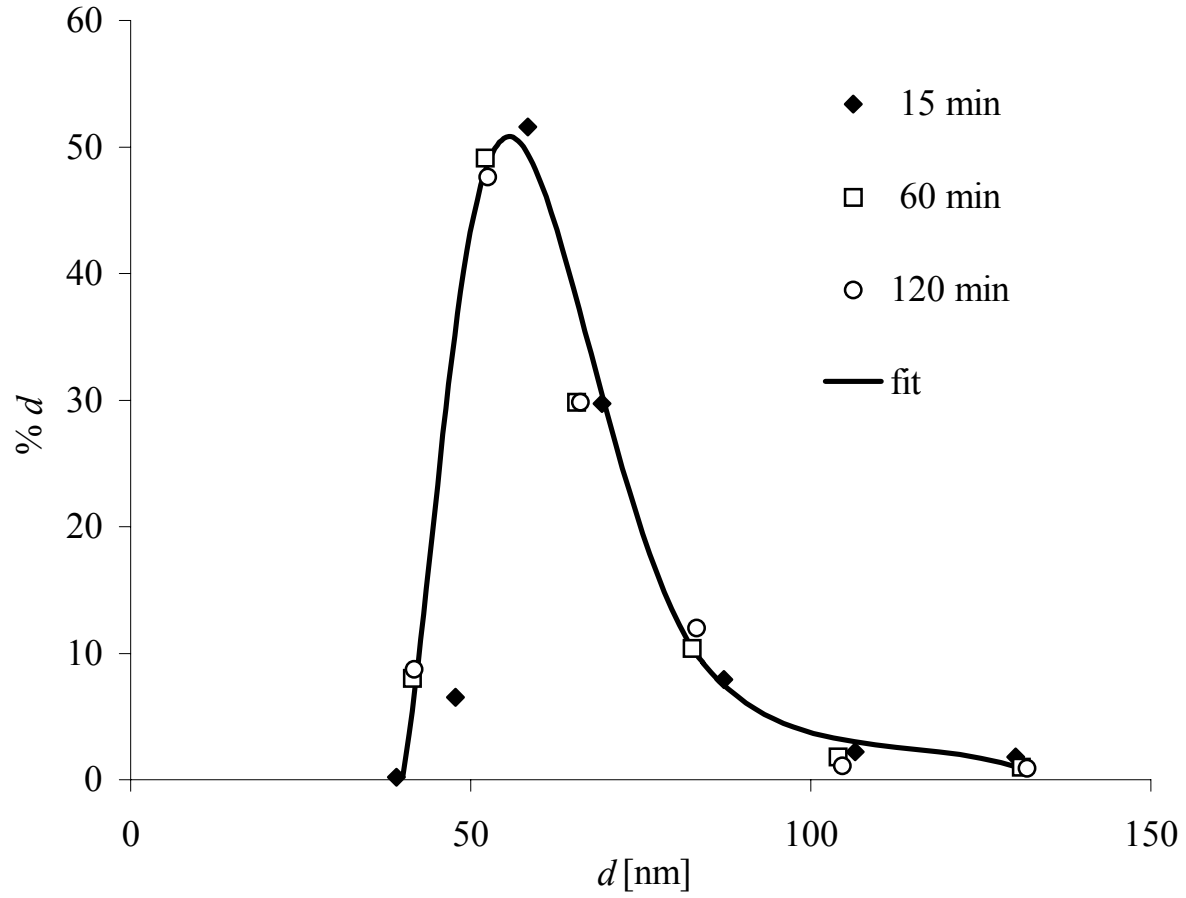


Figure 8-3: Particles size distribution observed during the polymerization of a microemulsion of styrene in water.

Atomic Force Microscopy and Transmission Electron Microscopy confirmed the size of the particles obtained using PCS. The observation using AFM and TEM does not only show particle size ranging from 50 to 100 nm as found in light scattering experiments but also gives information about the shape of the particle. Micellar particles in the region of microemulsion are spherical. During the polymerization, a deviation occurs in the shape of the particles and they become elongated. This deviation may be due to the following reasons: the changes of the oil phase thus, the composition of microemulsion region and the change of

the density from the monomer to polymer during the polymerization. A difference of up to 20 % is observed between the long and the short axes of the same particle. Figure 8-4 gives an idea of what is observed using AFM.

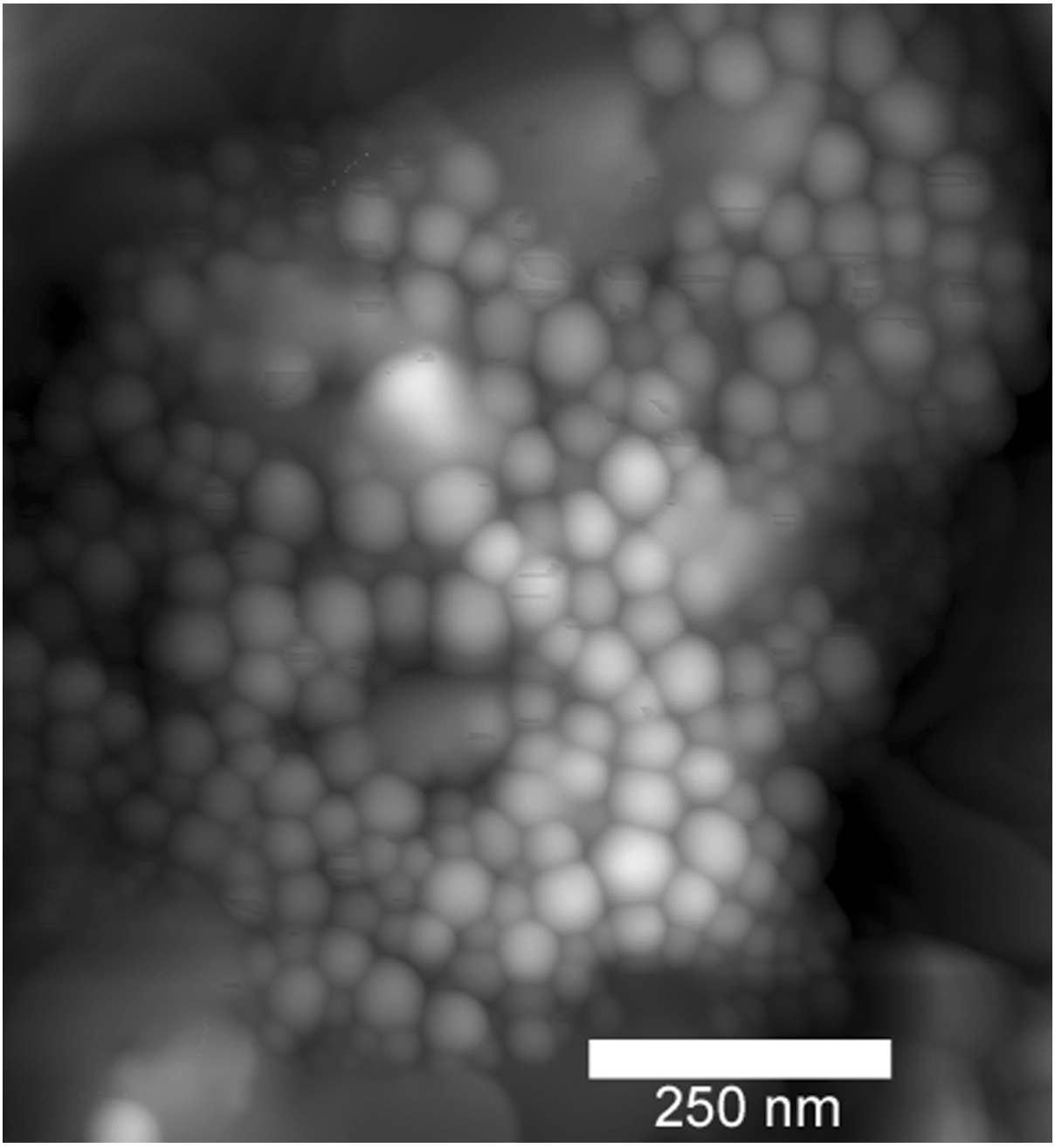


Figure 8-4: AFM images of latex particles

## 8.2 Polymerization with perylene as fluorescence probe

Before starting the investigation, it was necessary to observe the behavior of perylene before and during the polymerization. Especially no degradation or covalent bonding of the radicals or polymer to perylene has to be observed. The excitation and the emission spectra of perylene at $10^{-5}$ M in microemulsion at room temperature and during the polymerization of the microemulsion at 50°C are shown in figure 8-5. All spectra are normalized to maximal fluorescence intensity. No significant change is observed on the spectra of excitation before and during the polymerization. For emission spectra, the relative intensity changes and a small shift is observed at each maximum. Comparison of the emission and the excitation spectra before and after the polymerization leads to the conclusion that there are no specific interactions between the monomer or other ingredients of the microemulsion and the dye. It also shows that the dye remains stable at the reaction temperature.

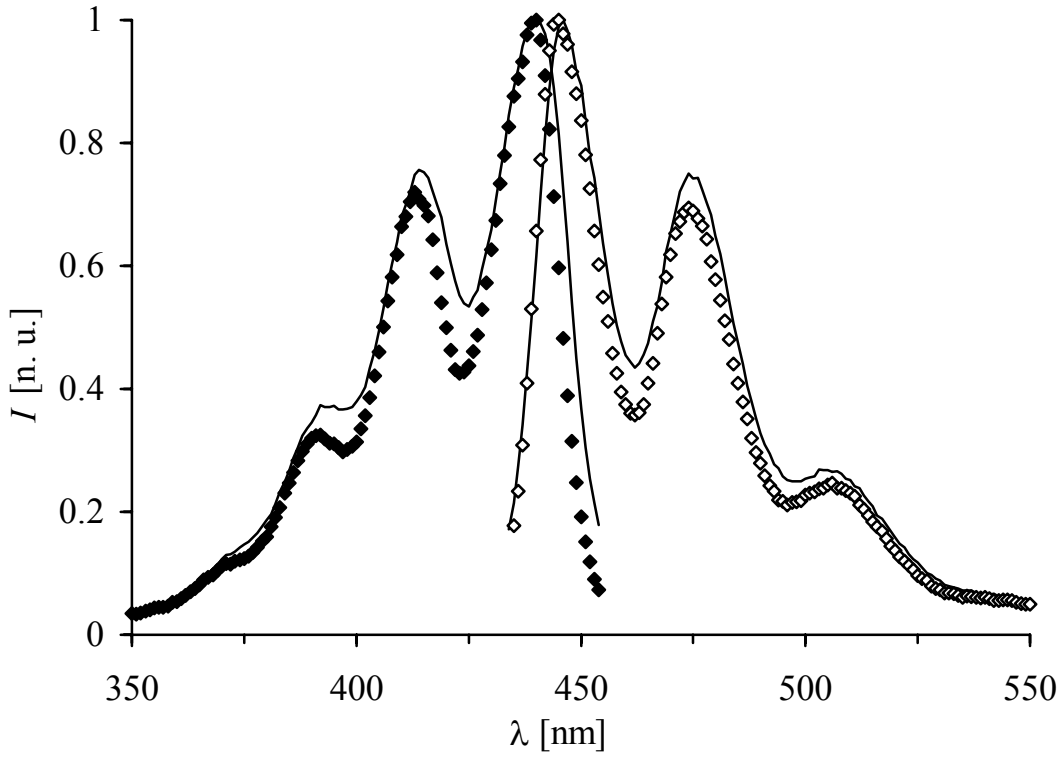


Figure 8-5: Excitation (♦) and emission (◊) spectra of perylene in microemulsion at 25°C. (—) is the excitation and emission spectra measured during the polymerization of microemulsion at 50°C.

### 8.2.1 Behavior of the intensities of scattering and fluorescence light

For the purpose of this investigation, not only the intensity of fluorescence is measured but also the intensity of pure scattering light at excitation and emission wavelength. As the polymerization goes on, the turbidity of the system increases and changes occur in the different intensities measured. Figure 8-6 depicts the plot of these intensities as a function of reaction time. These curves are obtained during the polymerization. The following explanations can be given to describe the changes observed in these curves.

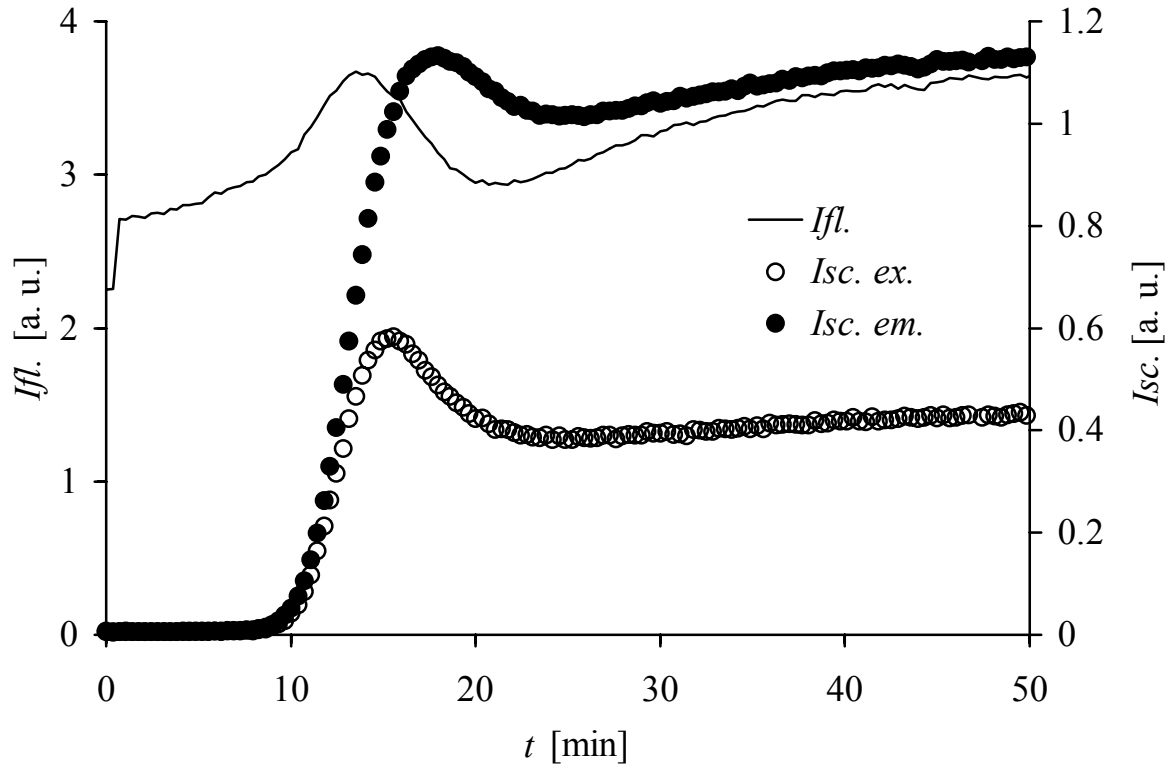


Figure 8-6: Intensities of fluorescence and scattering light as a function of reaction time in polymerizing microemulsion. The reaction temperature was 50°C and the concentration of perylene $10^{-5}$ mol/L. The reactor was a quadratic fluorescence cell and the reaction took place without stirring. The excitation and emission wavelength were $\lambda_{Ex}$ = 415 nm and $\lambda_{Em}$ = 474 nm.

As far as the intensities of scattering light are concerned, they start at zero because before the beginning of the polymerization, an induction period is needed and during this period, the system remains transparent. After the induction period (~10 minutes, depending on the individual polymerization), the number of the growing particles increases, leading to an increase in the intensity of scattering light up to a maximum at 15 and 17 minutes depending on the wavelength.

The decrease in the scattering light can be explained by investigating the intensity of the incident light from the light source in the volume of observation. With increasing number of scattering particles the intensity of the primary light in the observed volume decreases due to the increase in turbidity. Hence, the scattering intensity decreases. This effect depends on the scattering ability (scattering cross section) of the solution, which is wavelength dependant: the larger the wavelength, the lower the scattering. Depending on the polymerization conditions, this decay lasts for 10 to 15 minutes after which the intensities of scattering light at excitation and emission wavelength remain almost constant until the end of the reaction.

The plots of the intensities of scattering light as a function of reaction time are wavelength dependant. The difference in the behaviors of these plots starts when the size and the number of the polymerizing particles increase, that is, right at the beginning of the polymerization. At short wavelength (λ of excitation), scattering i.e. multiple scattering is stronger. This behavior can also be related to the change in the shape of the particles with time since the intensity of scattering light depends on it. It has to be considered that the scattering obtained from these measurements are not calibrated to a standard with a known *Rayleigh-ratio* and that they should therefore only be discussed regarding changes during the polymerization.

In contrast to the intensities of scattering and due to the transparency of the system, the intensity of fluorescence starts at relatively high value. After a short induction period compared to that shown by the intensities of scattering, the intensity of fluorescence increases. It reaches its maximum about 10 minutes after the beginning of the polymerization, then drops by around 75% of its maximum value for the next 10 to 15 minutes. After this period, the decay stops and the intensity of fluorescence slightly increases. The following reasons can be given to explain the behaviors of the intensity of fluorescence plots as a function of reaction time.

The increase in the intensity of fluorescence at the beginning of the reaction is related to the lifetime of the fluorophore, which is subjected to inhibition and quenching by residual oxygen molecule of the system. According to the Lambert-Beer law, the intensity of fluorescence is a function of the concentration of the fluorophore. The decay of the fluorescence intensity is due to the fact that a smaller number of fluorophores is excited because a great number of photons are scattered by increasing number of particles. This can be confirmed if the amplitude of the exponential decay used to describe the lifetime of fluorophore is considered. This amplitude is proportional to the excited number of dye whose emitted photons are actually detected. The plot (figure 8-7) of the amplitude as a function of reaction time increases up to a maximum then decays and later on remains constant until the end of the polymerization. The slight increase observed in the intensities of fluorescence and those of scattering light after the decay is mainly related to the polymerizing system and are not observed in each case.

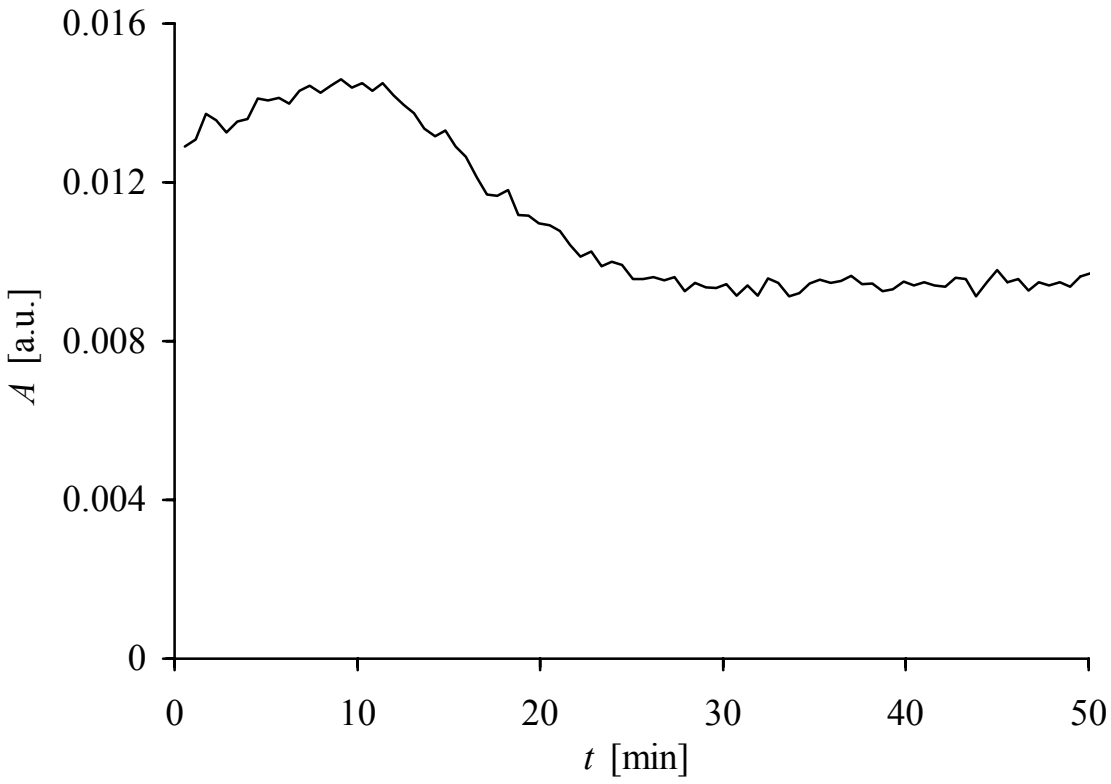


Figure 8-7: plot of the preexponential factor of the lifetime as a function of the reaction time.

Similar shape of the intensity-time curves has been observed by Loufty[21,23] and co-workers during the polymerization of MMA using [p-(N,N-dialkylamino) benzylidene]malonitrile 2 as fluorescent probe. They compared the fact that the intensity of fluorescence reaches its maximum with a certain conversion to the relationship between the limiting conversion and polymerization temperature proposed by Marten and Hamielec[30]. This was based on the fact that limiting conversion occurs at the point where the glass transition of the monomer/polymer equals the reaction temperature.

In the case of microemulsion polymerization of styrene using perylene as fluorophore, similar conclusions could not be drawn. In this system, the intensity of fluorescence is simply affected by the pure scattering due to an increase in the

number of particles leading to the change in turbidity. However, the microemulsion turns bluish at the end of the polymerization and is only slightly turbid. One has therefore to note that the degree of turbidity here remains acceptable and does not have an adverse effect on the data obtained from the experiment.

It is essential to observe that the maximum of the intensity of fluorescence nearly corresponds at the debut to the increase of the intensities of scattering. Starting at this point, the intensity of fluorescence behaves similar to those of scattering. This is due to the fact that fluorophores are mainly excited by the scattered photons. The changes in the intensities of scattering and that of fluorescence are related to the change of the properties of the polymerizing microemulsion amongst which the local viscosity.

The change of the local viscosity can well be observed if instead of looking at the intensities, one considers the anisotropy of fluorescence as well as those of pure scattering light at excitation and emission wavelength during the polymerization.

### 8.2.2 Determination of the anisotropies

The anisotropy is the parameter leading to the local viscosity. To determine these anisotropies, the vertical and perpendicular components ($I_{VV}$, $I_{VH}$, $I_{HH}$, $I_{HV}$) of the fluorescent and scattering light were measured online during the reaction. The anisotropies were calculated according to equation 4.3. Figures 8-8 and 8-9 show the spectra of perylene in microemulsion before and during the polymerization respectively.

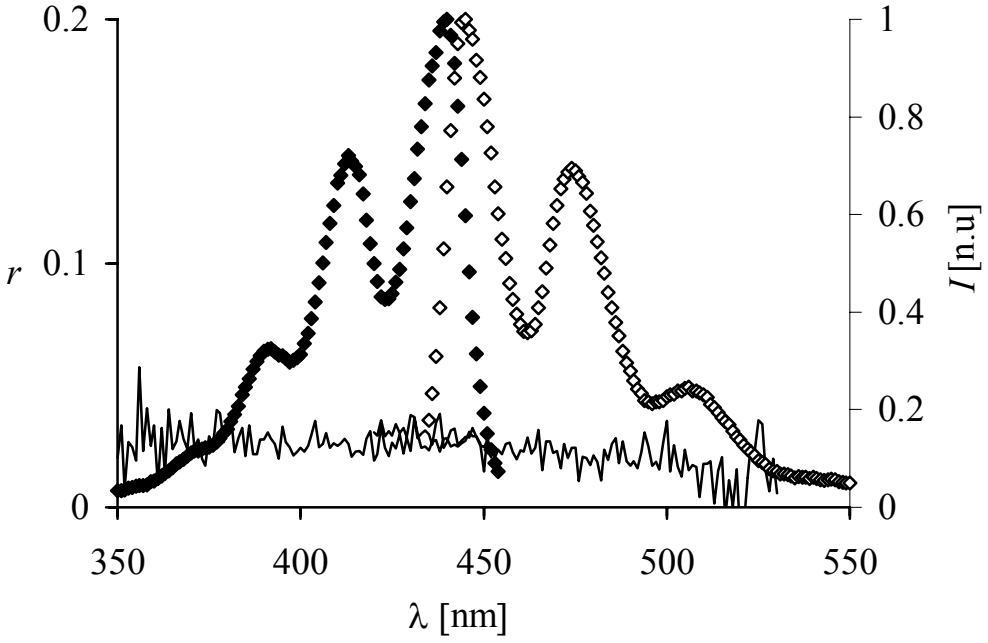


Figure 8-8: Excitation and emission spectra of perylene in microemulsion at 25°C (♦, ◊). (—) represents the anisotropy of excitation and emission light of perylene calculated from the intensities.

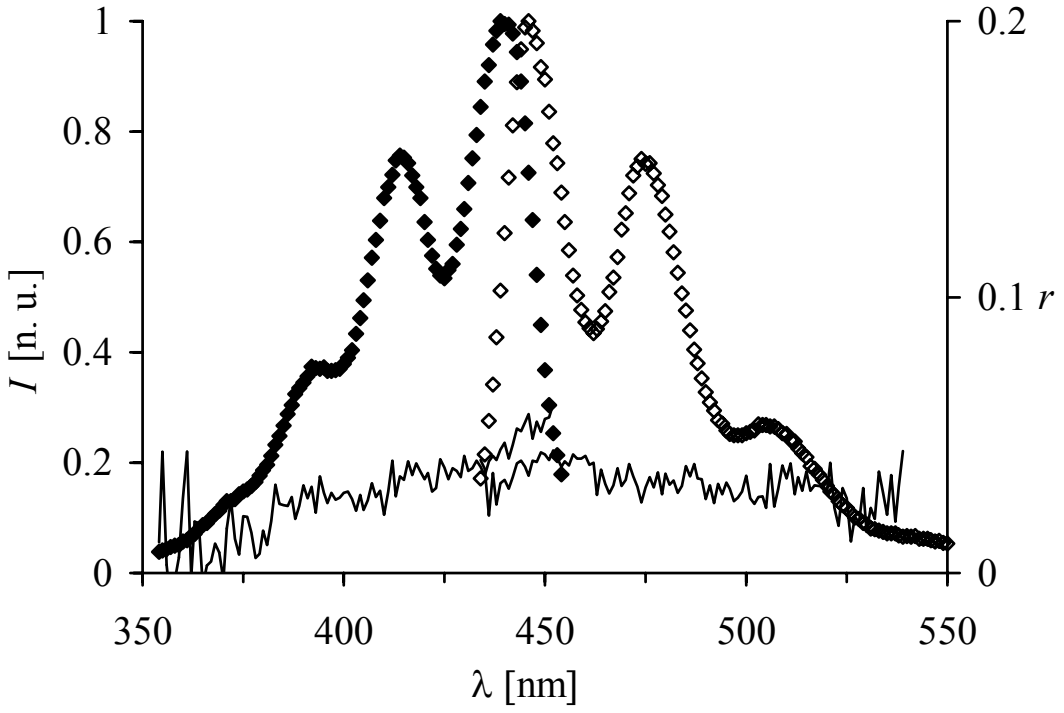


Figure 8-9: Excitation and emission spectra of perylene in a polymerizing microemulsion at 50°C (♦, ◊). The lines (—) are the anisotropies of excitation and emission light of perylene observed during the reaction and calculated from the intensities.

It is seen that the anisotropies of the dye in microemulsion at room temperature is constant and close to zero. In contrast to the anisotropies at room temperature, the anisotropies during the polymerization change with time characterizing changes in the properties of the microemulsion. The change in the anisotropy can be explained by the increase of the polymer fraction inside the polymerizing particle leading to the change in the optical properties of the microemulsion as will be shown later. Increasing the polymer fraction in the particle reduces the rotation of the dye leading to an increase in the anisotropy as will also be explained in the next section. The changes on the anisotropies during the course of the polymerization are well depicted by the anisotropy-time plot given in figure 8-10.

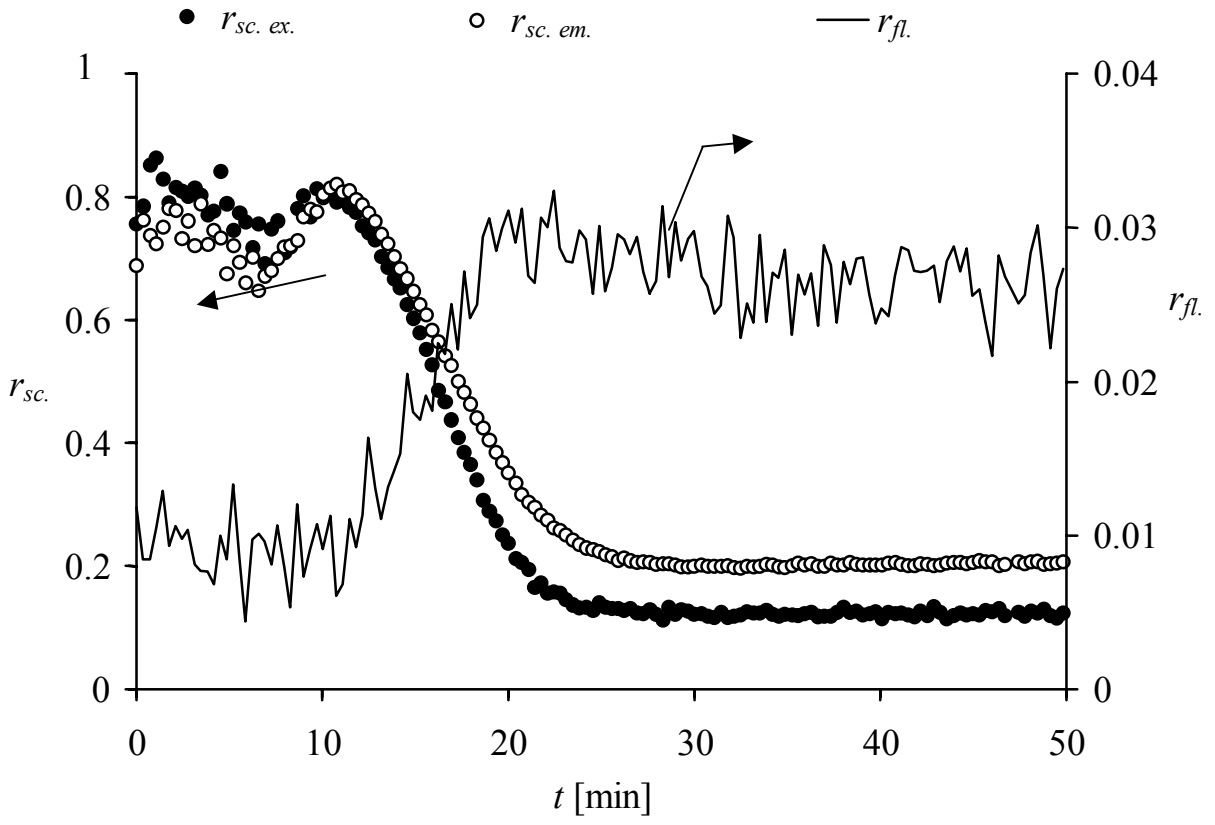


Figure 8-10: Anisotropy of fluorescence (—) and those of scattering at excitation wavelength (●) and scattering at emission wavelength (○) calculated from the observed intensity, using equation 3.3.

At a glance, the plots show an induction period, nearly the same for all the three plots. Between 10 to 25 minutes after the beginning of the polymerization, changes occur on the anisotropies-time plots and after that they remain constant until the end of the reaction.

The anisotropies of scattering start at relatively high value because no scattered particles are present in the medium.

The anisotropy of fluorescence increases by a factor of three during the polymerization but it is still very small to obtain a meaningful value of the local viscosity. This is the consequence of the multiple scattering effects. A correction of this phenomenon is needed in order to extract the fluorescence anisotropy, which will give information about the local mobility of the fluorescence probe.

As already shown (figure 8-2), the size of the particles changes very little, after 20% conversion, during the polymerization. The question as to whether or not the changes in the anisotropy can be used to describe the growth of polymer particles is left open.

### 8.3 Determination of the lifetime of the probe

Beside the anisotropy of fluorescence, the lifetime of the probe is also needed for our studies. The measurements of the lifetime are done by time resolved fluorescence spectroscopy and analyzed with a monoexponential fit curve.

A typical decay of the lifetime of fluorescent probe observed online during the polymerization of microemulsion at 50°C is shown in figure 8-11. The data of these plots were collected every 30 seconds.

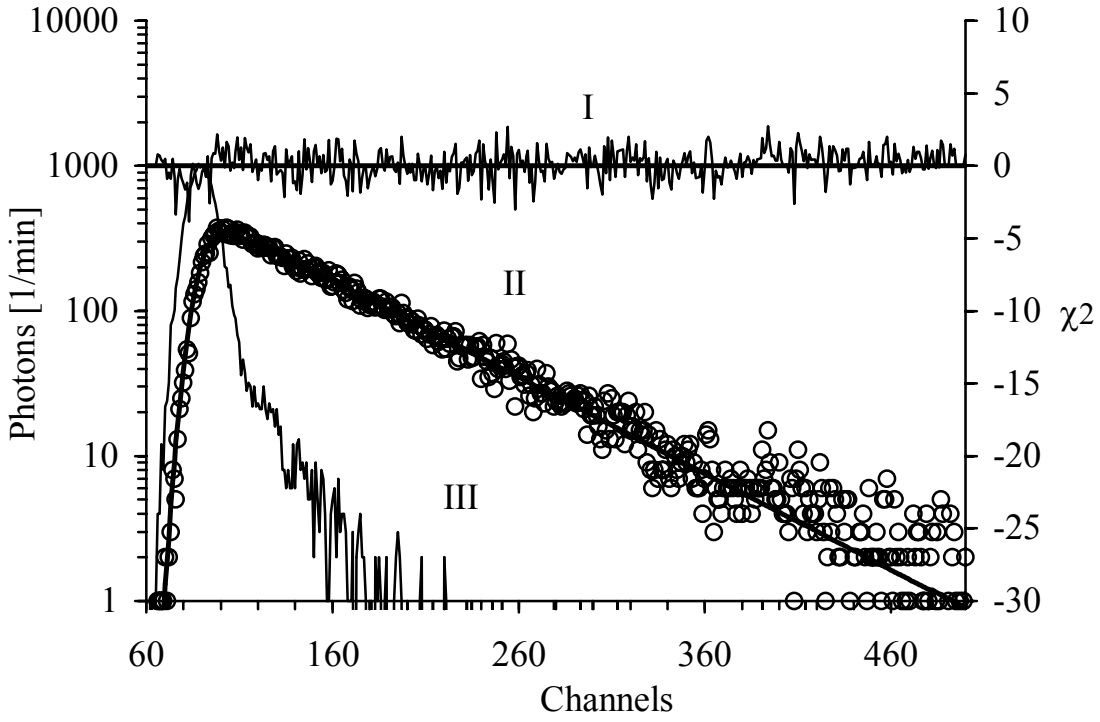


Figure 8-11: Fluorescence decay of perylene during the polymerization in microemulsion of styrene in water. Typical monoexponential decay is observed.

Curve I represents the percent residuals $\chi^2$ showing the quality of the fit. Curve II is the decay of the intensity of fluorescence of perylene and the fit superimposed on curve II is the calculated value $N(t_k)$ (equation 7.4 p. 42). The calculated decay assumes a single exponential decay. Curve III is the measured lamp pulse.

During the above experiment, a dilatometer was used to monitor the change in the fraction of polymer in the system. The aim was to correlate the change in the lifetime of perylene during the polymerization and the overall conversion of monomer to polymer.

Figure 8-12 depicts the plot of the conversion and the lifetime of fluorescence of perylene as a function of reaction time. The behavior of the lifetime is function of the concentration of quenching molecules. Three phases can also be seen on this graph:

Again an initial phase (0 to ~8 min) also known as induction period is observed. During this period the system is heated up to a desired temperature. A constant and low value of the lifetime of perylene is observed over a short period at the beginning of the polymerization. This lower value of the lifetime is mainly due to the presence of quenching molecules like residual oxygen. As the concentration of quenching molecules reduces, the lifetime of fluorescence increases.

After this period, a second phase (10 to ~ 25 min) in which, the conversion and lifetime increase in a parallel manner starts. The increase in the lifetime of perylene is mainly due to two factors, namely the change in the local environment of the probe and the rigidity of the system. The number of quenchers reduces with time and due to the rigidity of the system, the remaining quenchers diffuse with difficulty towards the fluorescent probe. The increase in

the rigidity of the system results in an increase in the polymer fraction inside the particle.

In the last phase (25 minutes and beyond), the lifetime reaches a plateau and it remains constant until the end of the polymerization. During a part of this period, the conversion continues to increase. It reaches its maximum at about 45 minutes and then remains constant until the reaction is stopped.

A comparative glance at the two curves suggests that it would be possible to obtain the different intervals of the mechanism of the microemulsion polymerization that are, as seen already: the induction period, the interval I and the interval II. However, one has to note that a shift is observed between the beginning of the increase in the lifetime and that of the conversion-time plot.

From the lifetime of fluorescence dye added into a polymerizing system, it may be possible to predict the conversion curve. An eye should be kept on this issue.

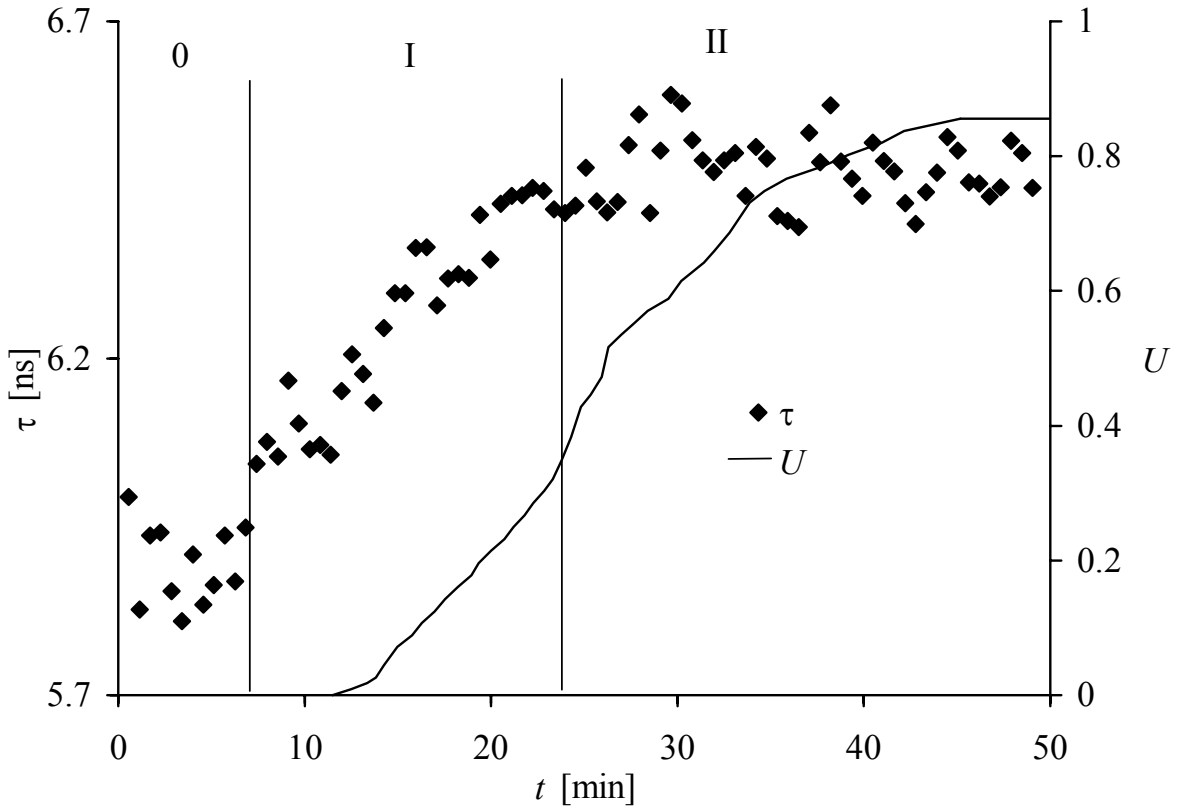


Figure 8-12: Lifetime (♦) of perylene and overall conversion (—) of monomer to polymer as a function of reaction time during the thermally initiated polymerization of styrene microemulsion.

The behavior of the fluorescent probe can well be understood if its lifetime measured during the polymerization is plotted as a function of the polymer fraction present in the system.

The plot of the lifetime of fluorescence as a function of conversion shown in figure 8-12 is divided into two regions. These regions are compared to the interval I and II of the mechanism of microemulsion polymerization.

During the interval I, the lifetime increases very slightly. This phenomenon occurs according to the curve of conversion, between 0 and 35 %. At these conversions, the rate of the polymerization reaction is maximal. The lifetime of the probe then reaches a plateau value after 35% conversion and remains almost constant up to the end of the reaction.

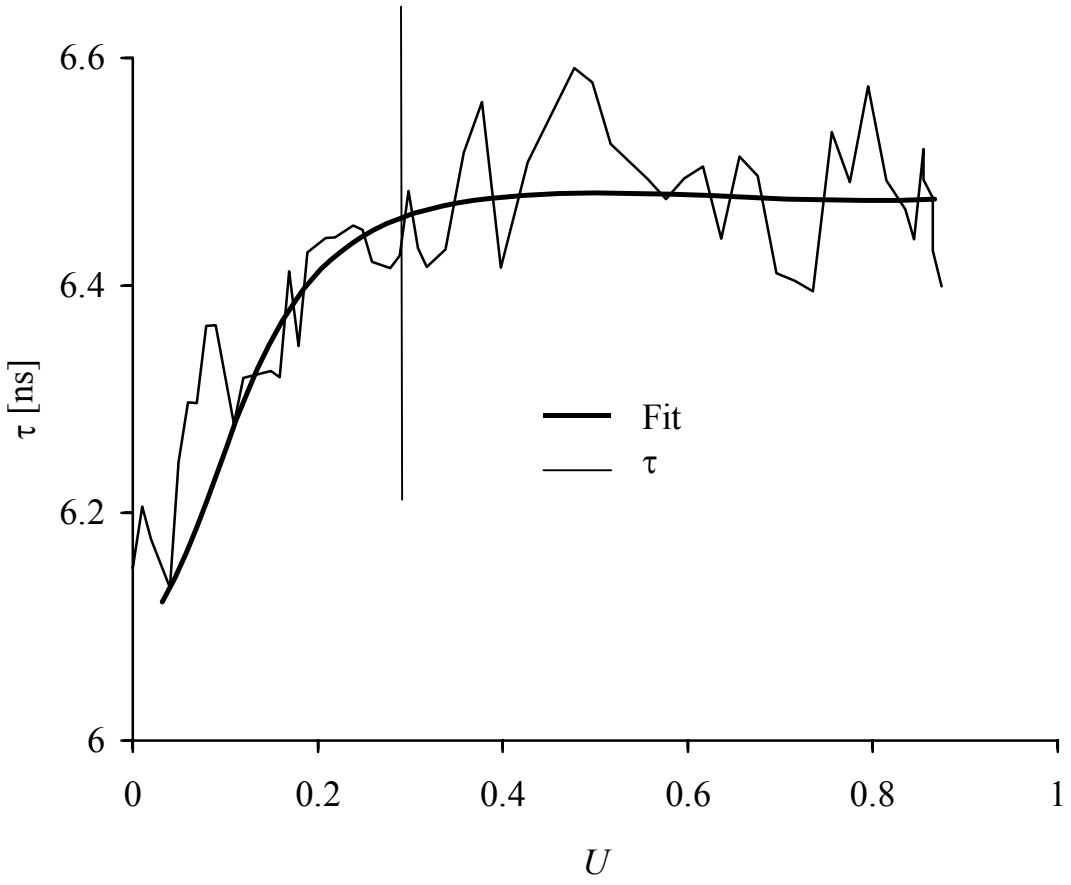


Figure 8-13: Lifetime (—) of perylene during the thermally initiated polymerization of styrene microemulsion as a function of the conversion.

One learns from figure 8.13 that the lifetime changes with the polymer fraction inside a polymerizing particle. The plot of lifetime as a function of the overall conversion assigns a lifetime of the fluorescent probe to each fraction of polymer. Like the polymerization process, the microemulsion became slightly turbid and the intensities of fluorescence and scattering light increase due to multiple scattering.

## 8.4 Multiple scattering in turbid media

The requirements for the comprehension, the characterization and the correction of the multiple scattering effects on the anisotropy are the studies of its dependency with respect to the concentration and the turbidity of the solution.

In order to avoid or reduce and to correct the impact of multiple scattering, it is important to know the extent to which this phenomenon affects the data obtained. In a series of experiments during which the concentration of the dispersion increases gradually, the intensities of fluorescence and scattering light are collected. The set up is fully computer-controlled and before collecting every data point, the mixture is stirred for 30 seconds. Figure 8-14 shows the intensities of fluorescence and scattering light at excitation and emission wavelength of perylene as a function of the dispersion concentration. It can be seen that the intensity of fluorescence increases continuously while those of scattering reaches a maximum and then decays.

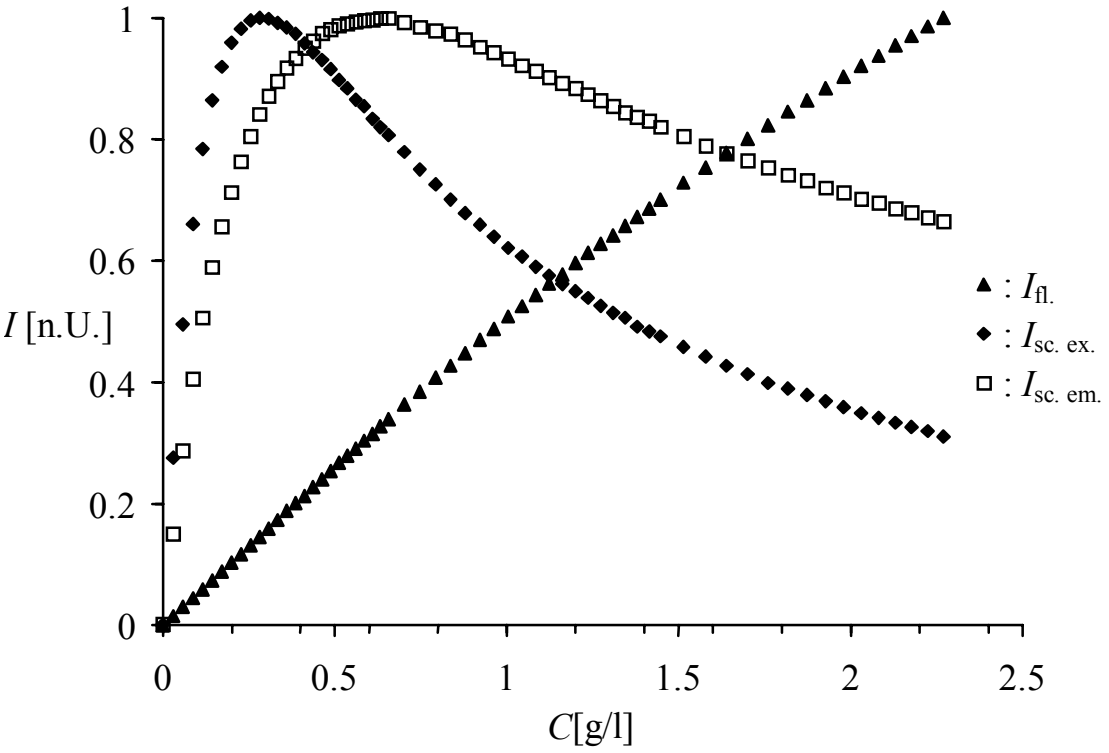


Figure 8-14: Measured intensities of fluorescence, $I_{fl.}$, and those of scattering at excitation, $I_{sc.\ ex.}$, and emission, $I_{sc.\ em.}$, wavelength as a function of PS-Perylene dispersion concentration.

The dependence of the anisotropy of fluorescence as well as those of scattering at excitation and emission wavelength on the concentration of the dispersion is shown in figure 8-15. It is deduced from the plot that increasing the concentration decreases the anisotropy of fluorescence. In the dispersion used for this experiment the probe is immobile in the polymer matrix. The depolarization of the fluorescence is then expected to be lower because there is no rotation of the probe. The decay of the anisotropies is essentially related to the growth of the turbidity of the system. This system will be used to test the model of correction of fluorescence developed so far. The aim will be to obtain a constant anisotropy with concentration.

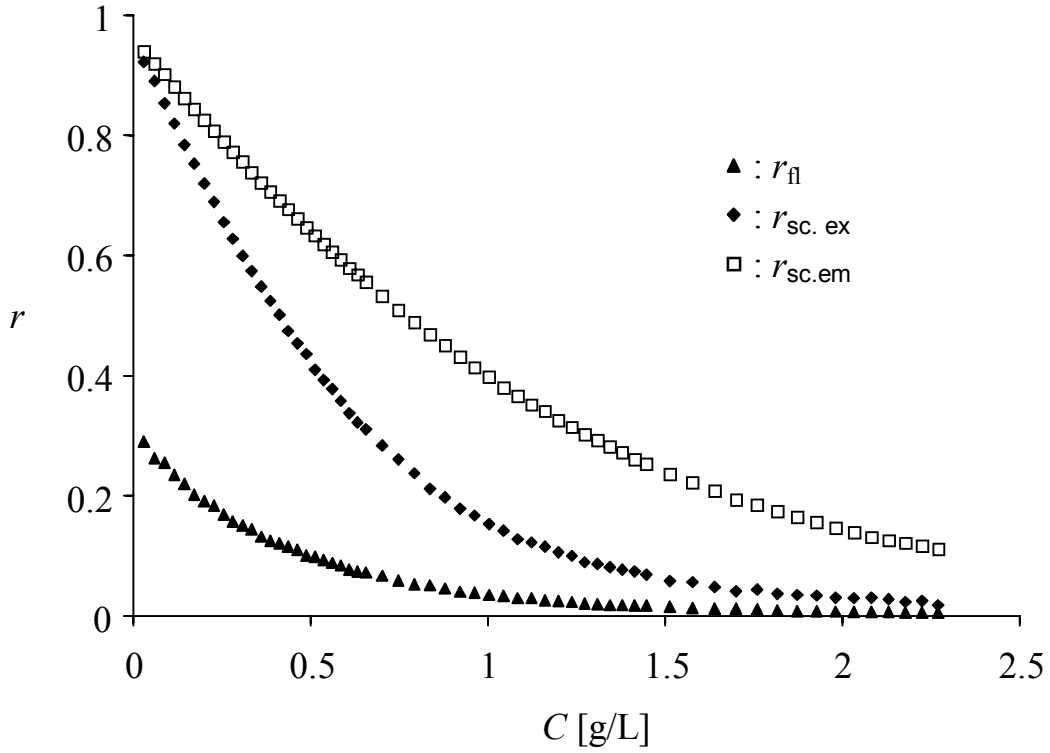


Figures 8-15: Measured anisotropy of fluorescence $r_{fl.}$ and those of scattering at excitation $r_{sc.\ ex.}$ and emission $r_{sc.\ em.}$ wavelength as a function of the dispersion concentration.

A semi-logarithmic plot of the anisotropies of this system as a function of concentration of the dispersion is shown in figure 8-16. This plot was done using equation (5.9) developed by Eisinger and Flores[83]. An extrapolation of the anisotropy of fluorescence at zero concentration, theoretically leads to the anisotropy observed without multiple scattering effects of the system. The value of the anisotropy of fluorescence obtained by the extrapolation is 0.3, which is close to the anisotropy of perylene in polystyrene phase as will be shown later. This result proves that no significant rotation of the dye occurs in Polystyrene phase. A similar extrapolation of the anisotropies of scattering should theoretically lead to a value 1. However, the result obtained is below 1, meaning that the anisotropy of single scattering is also depolarized. The depolarization due to the solvent molecules (water) is negligible and the only relevant factor of

the depolarization of scattering light is the shape of particle. As observed on AFM pictures, the particles are slightly elongated. A difference of about 20 to 30% is observed between the two perpendicular axes of a particle. The fact that particles are non spherical also plays a role in the depolarization of single scattering besides the multiple scattering.

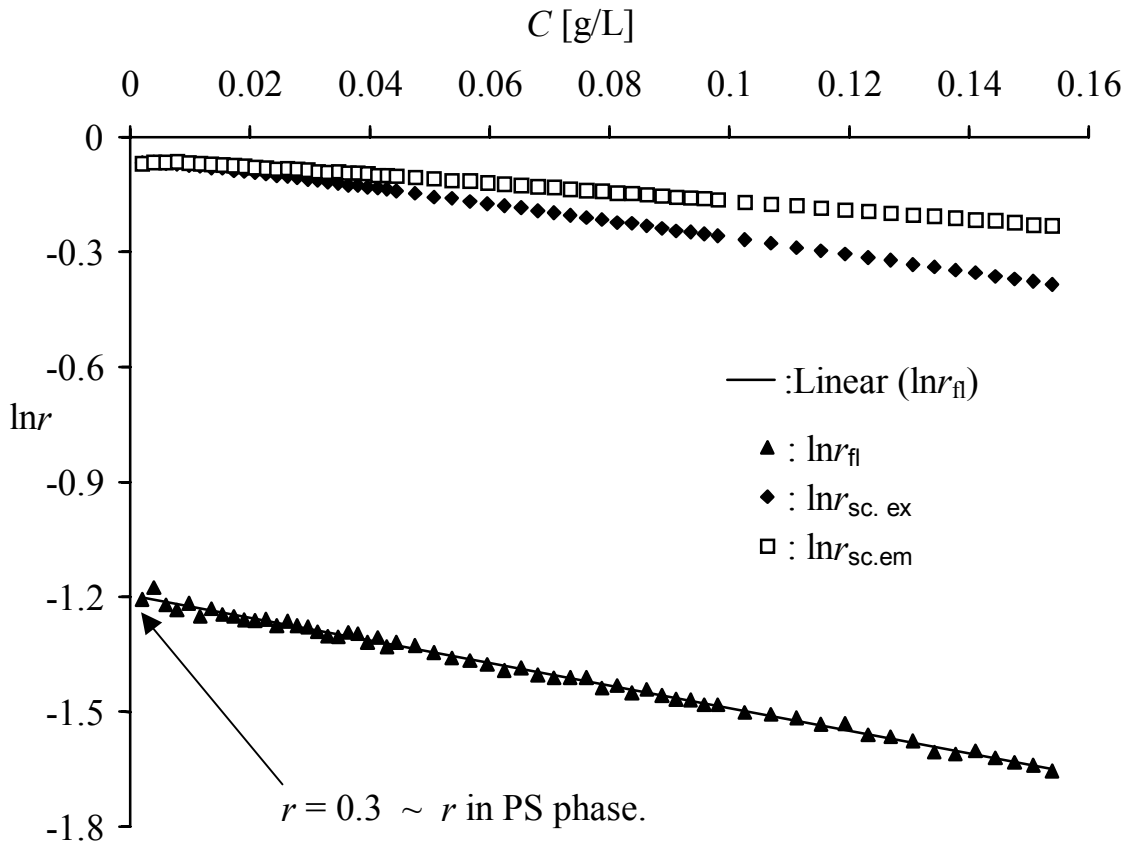


Figure 8-16: Logarithmic plots of the measured anisotropy of fluorescence $r_{fl.}$ and those of scattering at excitation $r_{sc.\ ex.}$ and emission $r_{sc.\ em.}$ wavelength as a function of dispersion concentration.

Another significant behavior observed in the semi-logarithmic (fig. 8-16) plot is the linearity between logarithms of *r* and the concentration. This linearity provides information about the location of the dye. It shows without ambiguity that the fluorescence dye is located in the same environment while increasing the concentration of the dispersion, that is, the hydrophobic region of the system. Even if the dye would have an equilibrium distribution between the water phase and the polymer particles, the ratio of the dye concentration in these two phases should vary according to Nernst's law when varying the concentration.

As shown in figure 8-15, the anisotropies decay with the increase of dispersion concentration. This decay was attributed to multiple scattering. A correction of the anisotropy will be done in order to use it for the evaluation of the local viscosity.

## 8.5 Correction of multiple scattering

The correction of the multiple scattering effects on fluorescence depolarization has been done for systems other than microemulsion polymerization. Teale[82] described in more general terms the depolarization of fluorescence light in scattering medium. Tsuneda[84] and co-workers did the correction of multiple scattering on the fluorescence anisotropy while investigating the local mobility of polymer chain grafted on polyethylene. The common factor on these studies was the fixed turbidity. The model of Tsuneda failed for our studies.

In this section, a correction of the multiple scattering in a polymerizing system will be applied. The correction equation (equation 8.1) is a modification from equation (5.10) developed by Tsuneda. This new model is based on the assumption that the paths of the photon before and after the excitation are equal. It takes into account the anisotropy of pure scattered light at excitation and emission wavelengths.

$$r = \frac{r'}{(r'_{ex.scat} \cdot r'_{em.scat})^{\kappa}} \qquad 8.1$$

A parameter $\kappa$ is introduced into this equation. This parameter contains the information about the position of the cell, the nature of the system and the wavelength of the excited and emitted light. The value of $\kappa$, which is between 0.5 and 1, is obtained from the slope of the curves of the logarithmic plot of $r$ versus concentration of the dispersion. Unfortunately the parameter $\kappa$ is function of the anisotropy itself and the position and the volume of the fluorescence cell. The information obtained by using this $\kappa$ parameter is the local viscosity. $\kappa$ changes with other parameters of the system meaning that the local viscosity is also affected. Keeping $\kappa$ constant is just an approximation. This issue makes the model of correction not so quantitative but rather qualitative.

Figure 8-17 shows the anisotropy of fluorescence as a function of the dispersion concentration corrected by this model. It is seen that the anisotropy of fluorescence has a constant value close to 0.33, the intrinsic anisotropy of the probe. Using this model in a diluted system, no dependency of the concentration on the anisotropy is observed thus leading to the conclusion that the model is able to correct the anisotropy of fluorescence in polymerizing microemulsion. In the next step, it will be applied to correct the anisotropy of fluorescence used to evaluate the local viscosity inside a particle.

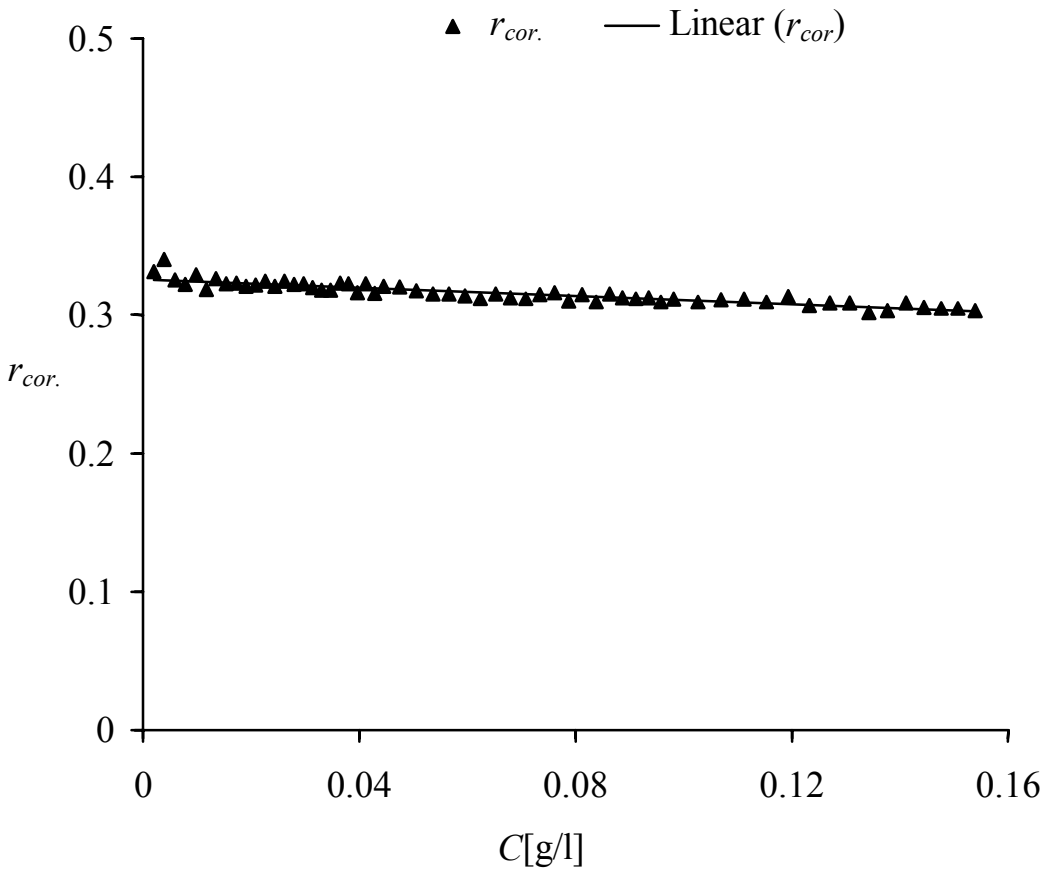


Figure 8-17: Corrected value of the anisotropy of fluorescence using the anisotropies of scattering respectively at excitation and emission wavelength.

For online polymerization, the anisotropies were deduced using the intensities measured and shown in figure 8-10. As already discussed, the change in the anisotropy of fluorescence is very small. Such a change does not lead to meaningful data of the local viscosity. These data can only be achieved if a correction is done to extract from the measured anisotropy, the amount of anisotropy indeed produced by rotational diffusion.

Using equation (8.1), a correction of the anisotropy of fluorescence obtained during the online polymerization of a microemulsion is given in figure 8-16. In

this figure, the anisotropies of scattering at excitation and emission wavelength are still represented.

A comparison between the value of the anisotropy of fluorescence in the plot obtained before the correction (figure 8-10) and that obtained after the correction shows an improvement in the data. The correction applied to the anisotropy leads to the conclusion that precedent results are multiplied almost by 10.

Again it is deduced that the corrected value of the anisotropy ($r_{cor.}$) is close to 0.3, the value obtained with the dispersion system, meaning that this model of correction can well be applied to investigate a polymerizing microemulsion online.

A strong increase in the anisotropy is noticed about 15 minutes after the beginning of the polymerization. Before 15 minutes, no relevant change occurs inside the polymerizing particles. After this period and within the next 10 minutes, the medium changes strongly. On a time conversion plot, this period corresponds to the time in which the rate of polymerization increases rapidly to reach a maximum. The anisotropy reaches a plateau at about 25 minutes and becomes constant up to the end of the reaction (fig. 8-18). At this time, the conversion is still far below 100%. The remaining monomer acts as a plasticizer leading to a small mobility of perylene.

During the same interval of time described above, the anisotropies of pure scattering light at excitation and emission wavelength, respectively, behave inversely to the anisotropy of fluorescence as can be seen in figure 8-18.

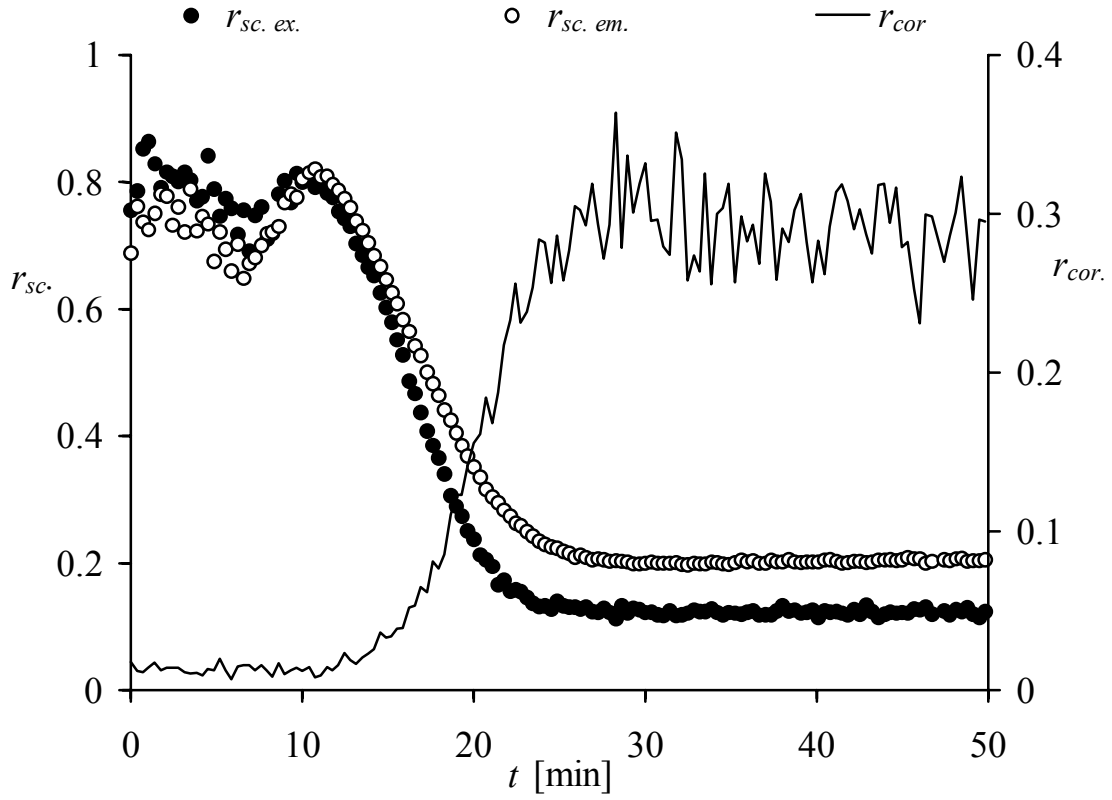


Figure 8-18: Corrected value of the anisotropy of fluorescence $r_{\text{cor.}}$ (—), $r_{sc.\ ex.}$ (●) and $r_{sc.\ em.}$ (○) are respectively the anisotropy of scattering at excitation and emission wavelength. All data points were measured during an on-line polymerization of a microemulsion.

The plot of anisotropy as a function of reaction time shows that the anisotropy of fluorescence remains constant after about 25 minutes, which is relatively early compared to the conversion in figure 8-1. This time is just an indication and can shift to ± 5 minutes depending on individual polymerization.

Since the anisotropy and the conversion of monomer to polymer were measured simultaneously, a plot of the anisotropy as a function of the conversion gives the value of the anisotropy at a given conversion. This plot is depicted in figure 8-19.

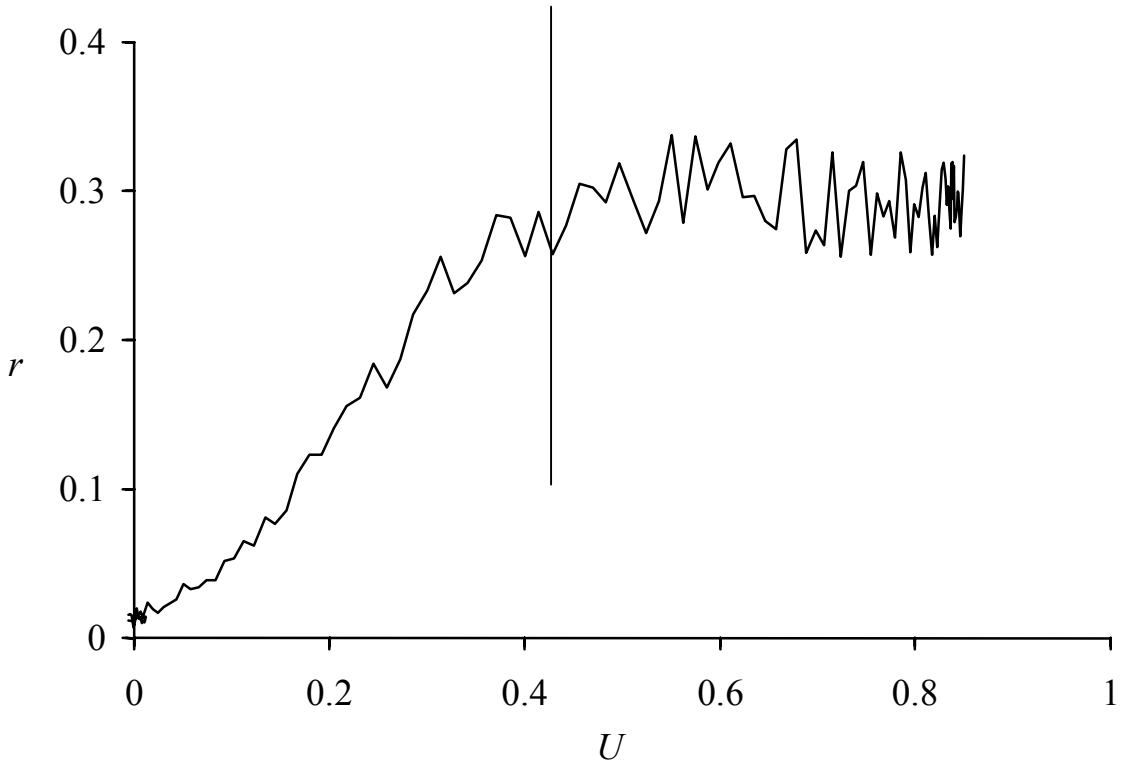


Figure 8-19: Corrected value of the anisotropy of fluorescence $r_{cor.}$ (—), as a function of the conversion of monomer to polymer.

The change of the anisotropy of fluorescence will be used to evaluate a qualitative change of the local viscosity inside a polymerizing particle in a microemulsion.

## 8.6 Determination of local viscosity inside a polymerizing particle

The local viscosity or microviscosity of a polymer system is determined by measuring the mobility of a small probe trapped in it. It gives information about the scale of the probe order i.e. dimension of a few *Å*. Thus the probe mobility is influenced only by a short section of the polymer, i.e. one or few monomer segments and not the entire chain.

The local viscosity or the microviscosity is determined by using the Perrin's equation given in equation (4.13) and which is restated here.

$$\eta = \frac{k \cdot T}{V_{hydro}} \cdot \tau \cdot \left( \frac{r_0}{r} - 1 \right)^{-1}$$

It does not only depend on the anisotropy but it is also a function of the lifetime of fluorescence. This lifetime is obtained by time resolved fluorescence spectroscopy while the anisotropy is deduced from the data collected by static fluorescence spectroscopy. The perrin's equation combines the data from polymerizations at different time and set ups. The only relation between these polymerizations is the conversion-time plot that behaves in the same manner. The anisotropy and the lifetime of the probe depend on the conversion. The plots in figure 8-13 and figure 8-19 assign to each value of the conversion a corresponding value of lifetime and anisotropy respectively. The knowledge of the lifetime and the anisotropy at a given conversion facilitates the use of the equation of Perrin to determine the local viscosity.

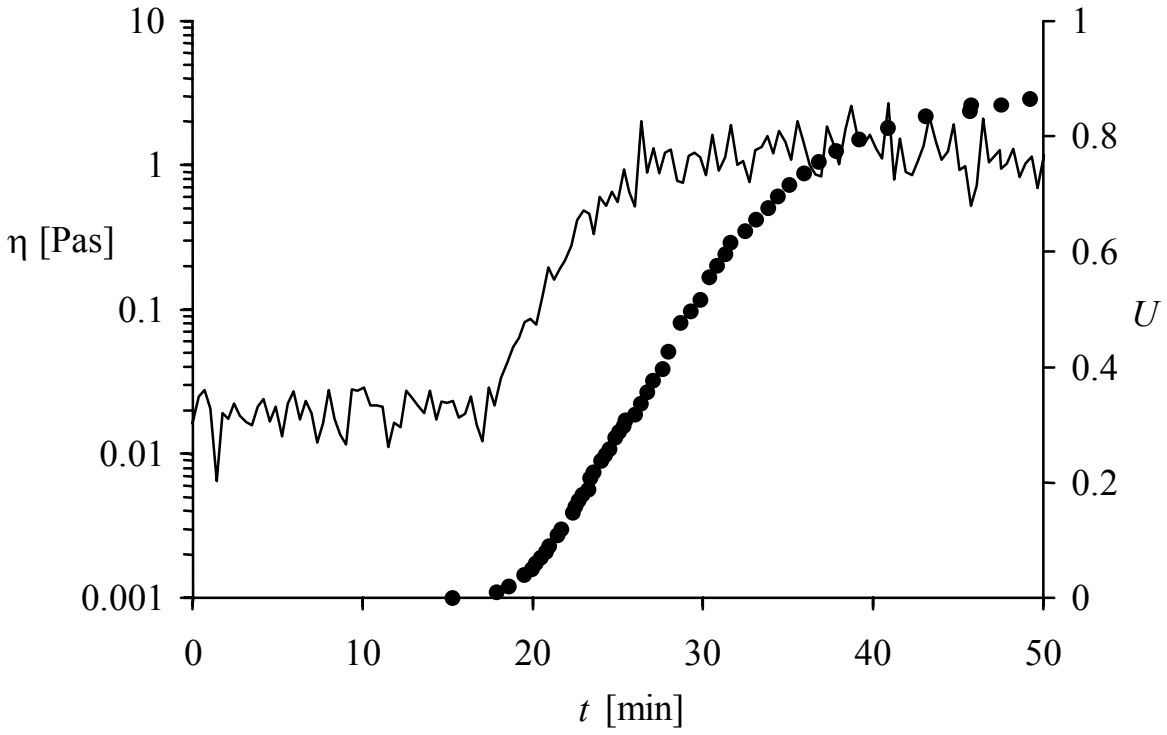


Figure 8-20: Calculated local viscosity η, (—) and overall conversion *U*, (●) measured during an on-line polymerization of a microemulsion.

Figure 8-20 shows the change of the calculated microviscosity and the conversion as a function of reaction time. At the beginning of the polymerization, the local viscosity is constant and low because only micelles filled with monomer exist. The probe dissolved in the monomer within these micelles has a high mobility. Between 15 to ~28 minutes, the polymer fraction (conversion) inside the polymerizing particles increases. The increase in the polymer fraction within the particles leads to an increase in the rigidity of the system. The local viscosity gradually increases leading to a continuous decrease in the mobility of the probe.

Above 30 minutes, the local viscosity remains constant up to the end of the process. At this period, the conversion time plot shows about 40 % conversion of monomer to polymer. At the same time, the rate of polymerization gradually

decreases (inset figure 8-1) because the concentration of monomer inside the particle decreases. Although the polymerization goes on, the sizes of the particles remain slightly constant until the end of the process.

The behavior of the local viscosity can be described by the nature of the microemulsion system. It is seen from the inset of figure 8-1 that the rate of polymerization goes up due to the increase in the number of polymerizing particle. The increase in the rate of polymerization ends up at 40% conversion. The distribution of the fluorescence probe between particles of different ratio of monomer-polymer fraction leads to the determination of an average value of the local viscosity.

As the polymerization proceeds, the increase in the polymer fraction inside the particles is observed leading to an increase in the local viscosity. The increase in the local viscosity between 0 and 40 % conversion may also be due to the increase in the number of polymerizing particles. At about 40% conversions, a high value of the local viscosity is measured. The local viscosity measured is that of the polymer dissolved in the remaining monomer swollen polymerizing particles since micelles vanish completely.

The change of local viscosity with conversion is shown in figure 8-21. It depicts the evolution of local viscosity as a function of the overall conversion. This plot shows that during the reaction, two regimes of local viscosity are observed. The first regime occurs at low conversions (1 to ~ 30%), where the local viscosity strongly increases. Between 1 and 10 % of conversion, the local viscosity changes from 0.02 to 0.16 Pas and at 29 % of conversion, it reaches the 1 Pas level. Knowing that at these conversions, the multiple scattering is negligible makes the technique suitable for the measurement of the local viscosity.

At about 40% conversion, the second regime starts and the values of the local viscosity oscillated between 1.3 and 1.7 Pas up to the end of the reaction.

It is interesting to note that the microviscosity reaches a saturated point where an increase in conversion has no effect on it. This phenomenon starts relatively early and the amount of monomer in polymerizing particles is still high (60%). A limiting value of local viscosity was also observed by Scarlata et al[89] while monitoring polymer cure using fluorescence depolarization. Other researchers[90-93] have pointed out the difference between the bulk viscosity (measured by mechanical experiments) and local or microviscosity experienced by fluorescent molecules in micelles or long-chained polymers. It has to be noted that most of these publications[90-93] discuss only the qualitative change in the microviscosity during the process. Therefore, interpretation of the plot 8-21 is more qualitative.

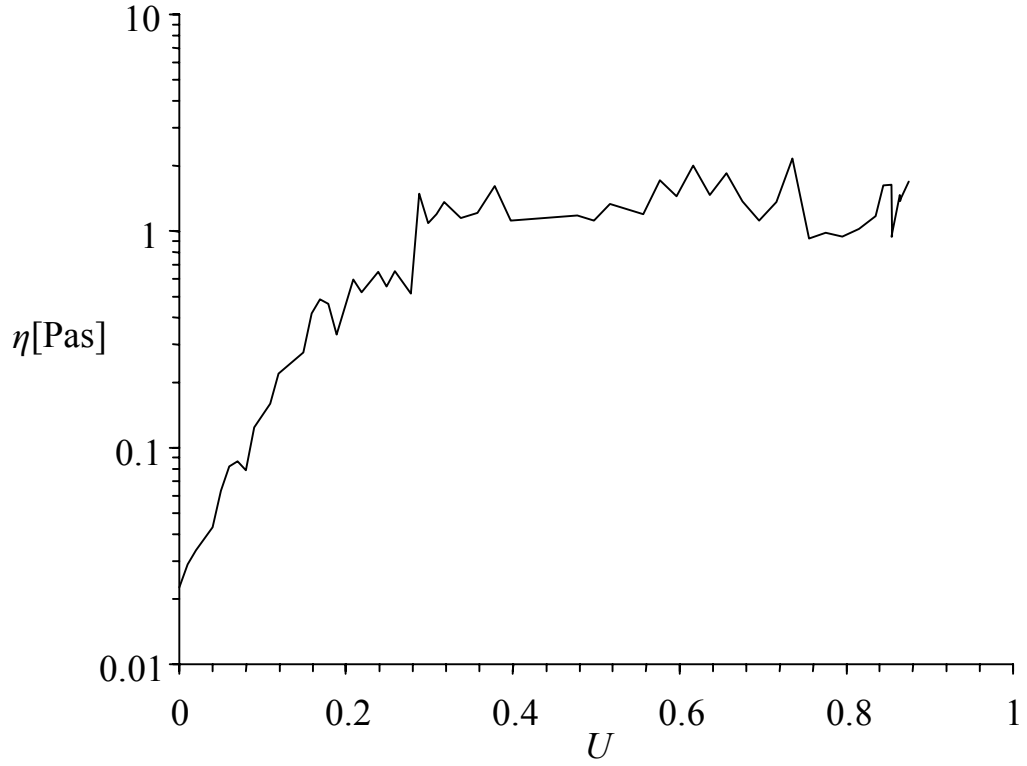


Figure 8-21: Calculated local viscosity (—) as a function of the overall conversion measured during an on-line polymerization of a microemulsion.

The average local viscosity measured by static fluorescence depolarization is of several orders of magnitude smaller than the macroviscosity of a polymer solution measured by a rheometer. These differences of magnitudes between

these values of the local and the macroviscosity are the proofs that these viscosities describe different behaviors of the material. The difference between the local or microviscosity and the macroviscosity is due to the fact that the rotation of perylene is influenced only by a short segment of the polymer chain compared to the macroviscosity where the entire chain of a polymer is concerned. This is the main reason why the values obtained are so small and are called local or microviscosity.

Using static fluorescence depolarization technique, it is not possible to distinguish between fully and partially polymerized particles. There is no possibility to obtain more information about the mobility of the dye and only an average mobility of the probe can be measured. The local viscosity determined is thus an average value from the different location of the dye. For a deeper analysis of the distribution of the rotational mobility of the probe, time resolved polarized fluorescence spectroscopy needs to be used.

# 9. Polymerization mechanism

The results of this work have shown that it is possible to obtain a correct change of the anisotropy of fluorescence of perylene in polymerizing microemulsion. From the corrected anisotropy, the change in local viscosity within polymerizing particles is determined. In this section, an attempt to interpret the changes in anisotropy in terms of polymerization mechanism is made. The aim of this section is not to study the polymerization process and behavior, but rather to show that beside the determination of physical parameters, it is possible, by using fluorescence depolarization technique, to predict the evolution of the reaction at least at low conversion.

For this purpose, the plot of the change of anisotropy as a function of reaction time given by figure 8-18 has to be considered. It can be divided into three domains 0, I and II.

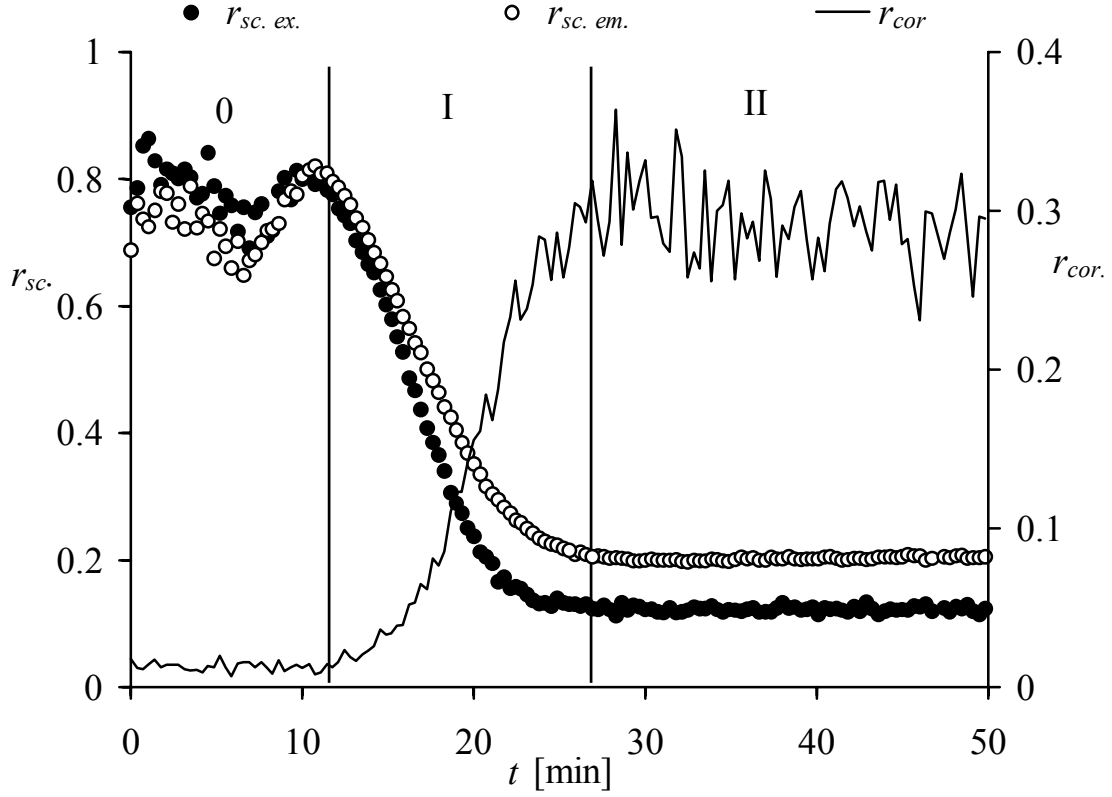


Figure 8-18: Corrected value of the anisotropy of fluorescence (—) calculated from the observed intensity, using equation 8.1 and the anisotropies of scattering at excitation (●) and emission (○) wavelength respectively.

The domain (0) on the plot is the induction period of the polymerization. During this period, radicals decompose and form oligomer radicals, which are adsorbed by the microemulsion droplets. The long induction period (10 to 15 minutes depending on the individual polymerization) observed here may be attributed to the shell structure formed by adsorption of surfactant and co-surfactant on the microemulsion droplets, which retards the rate of radical adsorption. The anisotropy of fluorescence is close to zero because perylene is dissolved into monomer and the microemulsion is still transparent. Until the end of this period, the amount of polymer already formed inside the particle is low and this explains the low value of anisotropy of fluorescence. This domain ends when the anisotropy of fluorescence starts to increase and those of scattering start to

decay. Usually this period is not mentioned in the microemulsion polymerization mechanism because in discussing the rate of polymerization versus conversion or time, it does not appear. For this reason, the mechanism of microemulsion polymerization is only discussed in terms of intervals I and II, represented here by domains I and II respectively.

Once inside the particle, the oligomer radical initiates the polymerization and the second domain (I) starts. It corresponds to interval I of the microemulsion polymerization. The particles grow by recruiting monomer micro droplets. As the polymer chain increases, the motion of the perylene molecules decreases.

The effect of an increase in polymer fraction on the anisotropy is well seen in this second domain of the plot in which an increase in the anisotropy of fluorescence is observed. It can also be observed on the plot of the anisotropy as a function of conversion. Anisotropy of fluorescence increases because the core of the particle becomes rigid with increasing polymer fraction leading to the reduction of the motion of probe. The strong increase in the anisotropy with conversion corresponds to the increase in the rate of polymerization between 20 to 30% conversion. At around 40% of conversion, the anisotropy reaches its maximum and remains constant whereas the polymerization continues. This can be seen on the plot of the anisotropy and conversion as a function of reaction time given in figure 8-18. The increase in the rate of polymerization measured by dilatometer passes through a maximum at this conversion and reaches zero before the polymerization is completed. As explained in the experimental part devoted to conversion measured by dilatometer, a long period of expansion is observed due to thermal equilibrium and inhibition. For small conversions (1 to 12%) measured by dilatometer value of the local viscosity between 0.01 to 0.1 Pas are determined.

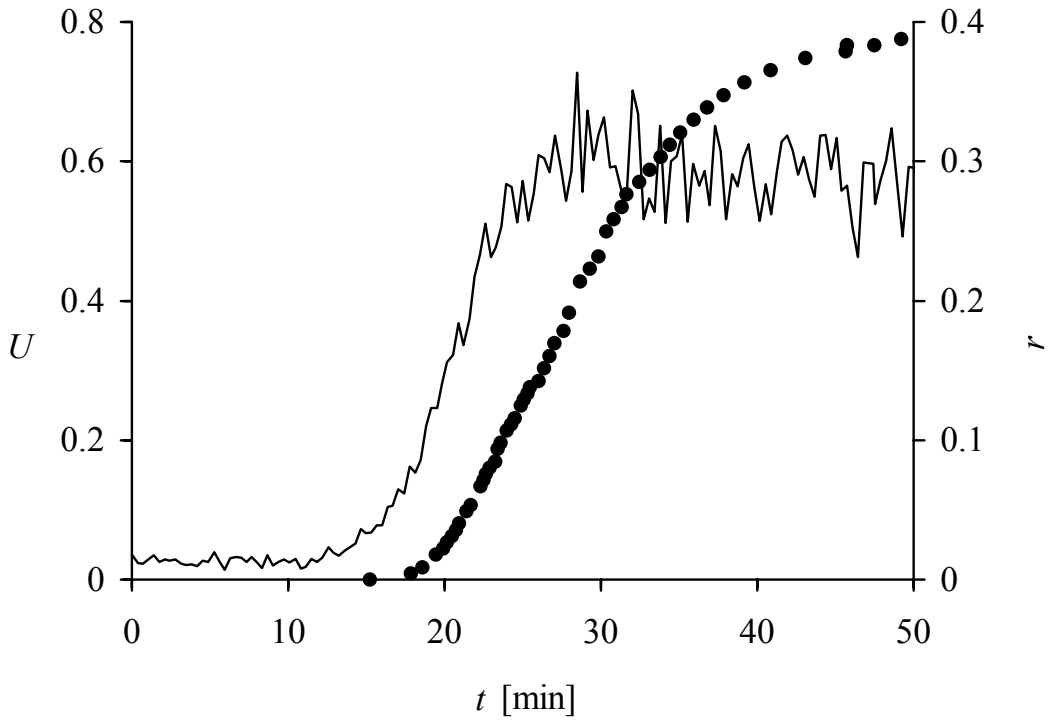


Figure 8-22: Corrected value of the anisotropy of fluorescence (—) and conversion (●) plot as a function of reaction time.

At the maximum point of the anisotropy, the third domain (II) of the plot commences. This domain also corresponds to the interval II of microemulsion polymerization and is characterized by a decrease in the rate of polymerization. In this domain, the anisotropy remains constant while the conversion increases up to its maximum value and then also remains constant up to the end of the polymerization. An increase in the polymer fraction inside polymerizing particles has no incidence on the anisotropy. This occurs at about 40% conversion. If one takes a look at the plot of the particle size as a function of the conversion, (figure 8-2), one notices that at nearly the same conversion, the particle size changes very slightly although the amount of polymer within the particle increases by consumption of monomer already inside the particle. A similarity is found in the behavior of the anisotropy and that of the polymer

particles leading to the question if there is a relation between the evolution of the particle sizes and the anisotropy of fluorescence.

However, as far as the beginning of the polymerization is concerned, the signal of the fluorescence spectroscopy and the dilatometer give different results. If the increase in the local viscosity marks the beginning of the polymerization then it may happen that the probe near the surface of the particle senses a change in its surrounding whereas only a very small change in volume is observed by dilatometer. The end of the polymerization is not clearly observed by the fluorescence technique because the local viscosity remains constant while a change in volume is still observed inside the dilatometer.

A contradiction is seen between the increase in the conversion and the constancy of the anisotropy of the fluorescence (thus the local viscosity) and the anisotropies of scattering at excitation and emission wavelength

## 10. Summary

This thesis presents the application of fluorescence depolarization to online monitoring of microemulsion polymerization. The subject covers a relatively broad range in chemistry: from luminescence to physical chemistry and from polymerization technique to polymer characterization. Therefore, a multi disciplinary approach was required to achieve the objective.

The first step in the line of this work was to choose the fluorescent dye to be used and to test it with a simple system like glycerol. Perylene, was chosen because of its photophysical properties and structure stability. Using glycerol at -5°C, the intrinsic anisotropy and the hydrodynamic volume of perylene were calculated.

The viscosity values of glycerol as a function of temperature found in literature were then compared to the values of viscosity obtained by fluorescence depolarization technique. The calculated values of the viscosity were in agreement with those in the literature. Although the viscosity of glycerol was temperature dependant, the perylene was stable at these temperatures and its lifetime remained constant. This allowed the heating of the mixture of glycerol and perylene to a suitable temperature. This was an important result, as it showed that the probe could be heated at few tens of degrees without any variation in structure and properties. At the end of this step, the partial conclusion is that fluorescence depolarization could in principle be used to determine the viscosity of transparent homogeneous systems.

The second step of this thesis was the study of the behavior of the anisotropy as a function of polymer dispersion concentration. A mixture of perylene and microemulsion was polymerized and the dispersion obtained was used for the investigation. A dilution series of this dispersion was done and at the same time, the intensity of fluorescence and the intensities of scattering light at excitation and emission wavelength, respectively, were collected. It was observed that the

intensities of scattering light left off at certain concentration while that of fluorescence continuously increased. From these intensities, the different anisotropies were calculated. The plots of the anisotropies as a function of the dispersion concentration show that perylene is located inside latex particles. It was also observed from these plots that the depolarization of the fluorescence might also be due to the particle shape. As the concentration of the dispersion increased, a decrease in the anisotropies was observed. This behavior was mainly attributed to the change of the optical parameters of the system and the multiple scattering related to it. Applying a correction method made it possible to obtain a constant anisotropy that does not depend on the concentration of the dispersion at least, at low concentration. The conclusion drawn at this step is that the multiple scattering and particle shape do not only depolarize the fluorescence light but also depolarize a single scattering light.

The next step of this research is to measure the anisotropy of fluorescence and pure scattering light during the online polymerization of microemulsion in order to deduce the microviscosity. This system is important if it is considered that, its turbidity changes with conversion. The goal of this step merges with the objectives of this thesis, which is the determination of the local viscosity inside polymerizing particles in emulsion. To determine the local or microviscosity, not only the anisotropy of the fluorescence probe is needed but also the lifetime of this probe. The lifetime of perylene is determined online by time resolved fluorescence spectroscopy. During this measurement, the conversion of monomer to polymer is also determined. This made possible the establishment of a correlation between lifetime of fluorescence and conversion. The plot of a lifetime as a function of conversion assigns to each fraction of polymer a lifetime necessary to obtain a local viscosity at this conversion.

Using static polarized fluorescence spectroscopy, the anisotropy of fluorescence as well as those of scattering at excitation and emission wavelength are determined. It is shown that the multiple scattering effects affect the change of

the anisotropy of fluorescence. This multiple scattering effect significantly reduces the obtained anisotropy. The effect of the multiple scattering is corrected. The correction equation takes into account the anisotropy of scattering at excitation and emission wavelength. It contains a parameter κ, which is a function of the fluorescent cell, its position as well as the system. Applying this correction equation leads to the value of the anisotropy needed to determine the microviscosity.

During the online measurement of the anisotropies, the conversion of monomer to polymer is simultaneously measured. The aim of this is to assign at each value of anisotropy, a corresponding value of the conversion in order to use lifetime and anisotropy in the Perrin's equation. The conversion measured during different experiments (time resolved and static fluorescence) has similar behavior when they are plotted as a function of time. They also depend on individual polymerization so various starting points are observed.

The anisotropy and the lifetime of the fluorescent probe at each conversion are known and can then be used to calculate the local viscosity.

The results of the thesis clearly demonstrate that the fluorescence depolarization technique is a good tool for online investigation of the local properties of polymerizing microemulsion system. Moreover, the combination between fluorescence depolarization and dilatometer experiments has a considerable advantage insofar as that makes it possible to follow the kinetics of the polymerization.

Some discrepancies were observed between the data from the dilatometer and the signal of fluorescence concerning the beginning and the end of the reaction.

By an appropriate choice of the fluorescent probe, the dynamics of heterogeneous system at nano-time scale can be observed. With a good optimization of the parameters of the set up, fluorescence depolarization

technique can in future be a good tool for online investigation of several systems not only for academia but also for industries.

# 11. References


1. B. Jönsson, B. Lindman, K. Holmberg, B. Kronberg; „ *Surfactants and polymers in aqueous solution*“, John Wiley & Sons, Chichester, (1998)
2. G. Odian; *Principles of Polymerization*, McGraw-Hill 279 (1970)
3. D. R. Bassett, A. E. Hamielec; “*Emulsion polymers and Emulsion Polymerization*”, ACS Symp. Ser., 165 (1981)
4. J.M. Asua; “*Polymeric Dispersion: Principles and Application*”, Kluwer Academic Publisher (1997)
5. R. G. Gilbert; “*Emulsion Polymerization: A Mechanistic Approach*” Academic Press London (1995)
6. M. Nomura, K. Suzuki, *Macromol. Chem. Phys.*, **198**, 3025 (1997)
7. M. Antonietti, R. Basten, S. Rohmann, *Macromol. Chem. Phys.*, **196**, 441 (1995)
8. K. Suzuki, A. Goto, M. Takayama, A. Muramatsu M. Nomura, *Macromol. Symp.*, **155**, 199-212 (2000)
9. F. Candau, P. Bucert, *Colloids and Surfaces*, **48**, 107 (1990)
10. I. Capek *Adv. Colloid and Interface Sci.*, **82**, 253 (1999) and references therein
11. J. E. Puig, V. H. Peréz-Luna, M. Peréz González, E. R. Macías, B. E. Rodriguez, E. W. Kaler, *Colloid Polym. Sci.*, **271**, 114 (1993)
12. Mamoru Nomura and Kiyoshi, *Colloid and Surface Sci*.: *part A*, **153**, 23 (1999)
13. J. M. Cowie, *Polymers: Chemistry and Physics of Modern Materials;* p.55, 2nd Ed, 1991
14. C. C. Co, R. de Vries, E. W. Kaler, *Macromolecules*, **34**, 3224, 3233, 3245, (2001)

15. N. Girard, Th. F. Tadros, A. I. Bailey, *Colloid Polym. Sci*., **276**, 999 (1998)

16. B. G. Manders, J. Sarnecki, Alex M. van Herk et al., *Makromol. Chem., Rapid Commun.*, **14**, 693 (1993)

17. I. Capek, P. Potisk, *Macromol. Chem. Phys.*, **196**, 723 (1995)

18. S. Holdcroft, J. E. Guillet, *J. Polym. Sci*.: *Part A*, **28**, 1823 (1990)

19. C. Decker, K. Moussa, *Makromol. Chem*., **191**, 963 (1990) and *Macromolecules*, **22**, 4455 (1989)

20. A. P. Full, E. W. Kaler, J. Arellano, J. E. Puig, *Macromolecules*, **29**, 2764 (1996)

21. R. O. Loutfy, *J. Polym. Sci*.: *Part B*, **20**, 825 (1982), R. O. Loutfy, *Macromolecules*, **14**, 270 (1981)

22. C. Yoshiki, I. Tomita, T. Saegusa, *Macromolecules*, 23, 689 (1990)

23. R. O. Loutfy, *Pure Appl. Chem.*, **58**, 1239 (1986)

24. J. Paczkowski, D. C. Neckers, *Macromolecules*, **25**, 548 (1992),

25. J. Paczkowski, *Macromolecules*, **24**, 2172 (1991)

26. O. Valdes-Aguilera, C. P. Pathak, D. C. Neckers, *Macromolecules*, **23**, 689 (1990)

27. M. Han Chung; *Dissertation*, TU Clausthal (1997)

28. G.B. Bahera et al., *Adv. Colloid int. Sci.*, **82**, 1(1999)

29. S. F. Scarlata, J. A. Ors, *Polym. Com*., **27**, 41 (1986)

30. F.W. Wang, R. E. Lowry and B. M. Fanconi, *Polymer*, 27, 1529 (1986)

31. P. A. Lovell, M. S. El-Aasser; "*Emulsion polymerization and Emulsion Polymers*", John Wiley & Sons, Chichester, (1997)

32. I. Capek, *Adv. Colloid and Interface Sci.*, **80**, 85 (1999)

33. D. W. Harkins; *j. Am. Chem. Soc.*, **69**, 1428-1445 (1947)

34. W. V. Smith, R. H. Ewart; *J. Chem. Phys.*, **16**, 592-599 (1948)

35. I. Piirma; "*Emulsion polymerization*", Academic Press, New York (1982)

36. K. E. J. Barrett, *Dispersion Polymerization in Organic Media*, John Wiley & Soons: London 1975

37. F. Candau, R. H. Ottewill; *An Introduction to Polymer Colloids*, Kluwer Academic Publishers 1990

38. G. W. Poehlein, in *Polymeric Dispersion: Principle and Applications*, J. M. Asua (Ed.), Kluwer Academic Publishers (1997)

39. J. B. P. Soares, A. E. Hamielec, in *Polymeric Dispersion: Principle and Applications*, J. M. Asua (Ed.), Kluwer Academic Publishers (1997)

40. S. H. Shen, S. L. Chiang, R. Strey, *J. Chem. Phys.*, **93**, 1907, (1990)

41. J. S. Guo, M. S. EL-Aasser and J. W. Vanderhoff; *J. Polymer Sc: Part A*, **27**, 691-710 (1989)

42. P.L. Johnson, E. Gularim, *J. Polym. Sc. Poly. Chem.*, **22**, 3967, (1984)

43. J. Barton, *Prog. Polym. Sci.*, **21**, 399 (1996)

44. Y. S. Leong, F. Candau, *J. Phys. Chem.*, **86**, 2269 (1982)

45. Inverse microemulsion

46. J. F. Rabek; "*Experimental Method in Photochemistry and Photophysics*", Part I & II, john Wiley & Sons (1982)

47. A. J. Pesce, C. G. Rosén, T. L. Pasby, "*Fluorescence Spectroscopy: An Introduction for Biology and Medicine*", Marcerl Dekker Inc. New York (1971)

48. J. R. Lakowicz; "*principles of fluorescence Spectroscopy*", Pleum Press: New York (1983)

49.K. Kalyanasundaram, in "*Photochemistry in Organized and Constrained Media*", V. Ramamurty (ed), Ch. 2, 39 (1991)

50.L. Alexandru, A.C. Somersall, *J. Polym. Sci*., **15**, 2003, (1977)

51.I. Mita, K. Horie, *Polym. J.*, **9**, 201, (1977), S. E. McGraw, *J. Polym. Sci*.: *Part B*, **8**,1323 (1970)

52.H. Morawetz, *Science*, **203**, 404 (1979)

53.Y. Nishijima, *J. Polym. Sci*.: *Part C*, **31**, 353 (1970)

54.S. W. Beaven et al, *Adv. Photochem.*, **11**, 207 (1979)

55.J. Easteo, B. H. Robinson A. J. W. G. Visser and D. C. Steytler, *J. Chem*. *Soc. Faraday Trans.*, **87**, 1899 (1991)

56.G. Oster, Y. Nishijima, *J. Am. Chem. Soc.*, **78**, 1581 (1956)

57.Linda B. McGown, Kasem Nithipatikon, *Applied Spec. Rev*, 35(4), 353-393 (2000)

58.G. Weber, *J. Chem. Phys*., **55**, 2399 (1971)

59.D. I. Bower, *J. Polym. Sci*. *Part B*, **10**, 2135 (1972)

60.B. Valeur, L. Monnerie, J.P. Jarry, *J. Polym. Sci*.: *Part B*, **13**, 675 (1975)

61.P. Wahl, *J. Polymer Sci.*, 29, 375 (1958)

62.A. J. W. G. Visser et al. *J. Phys. Chem*., **92**, 759 (1988)

63.R. A. Kenner, A. A. Aboderin, *Biochemistry*, **10**, 4433 (1971)

64.J. Henry Pownal, Louis C. Smith, *J. Am. Chem. Soc.*, **95,** 16, (1973)

65.Y. Nishijima *J. Polym. Sci*. *Part C*, **31**

66.S. Tazuke, M. A. Winnik in "*Photophysicals and Photochemical Tools in Polymer Science*", M. A. Winnik (ed) 37 (1986)

67.Keiko Ono, K. Ueda, et al., *Macromolecules*, **29**, 1584 (1996)

68.K. Brown, I. Soutar; *Eur. Polym. J*., **10**, 433 (1974)

69. D. A. Waldow, M. D. Ediger, Y. Yamaguchi, Y. Matsushita, I. Noda; *Macromolecules*, **24**, 3147 (1991)

70. J. Michl, E. W. Thulstrup; "*Spectroscopy with Polarized Light*", VCH Publishers, Inc. (1995)

71. A. Szabo; *J. Chem. Phys*., **81**, 150 (1984)

72. F. Perrin; *Ann. Phys*., **12**, 169 (1929)

73. D. Farrington, R. A. Albertz; "*Physical Chemistry*", 3rd Ed. J. Wiley & sons Inc. P.685, (1961)

74. M. Kerker; "*The Scattereing of Light and other Electromagnetic Radiation*", Academic Press, New York (1969)

75. R. Pecora; "*Dynamic Light Scattering: Application of Photon Correlation Spectroscopy*", Plenum Press, New York (1985)

76. Lord Rayleigh; *Nature*, **3**, 243 (1871)

77. G. Mie; *Ann. Phys.*, **25**, 377 (1908)

78. J. R. Parington; "*An advanced Treatise on Physical Chemistry*" v. 4 Physico-Chemical Optics, pp. 240-253, (1967)

79. M. Shinitzky A. Dainoux, G. Gitler,G. Weber, *Biochem.*, **10**, 2106 (1971)

80. B. R. Lentz, B. M. moore, D. A. Barrow; *Biophys. J.*, **25**, 489 (1979)

81. J. Adams; *Habilitationsschrift*, Technische Universität Clausthal (1999)

82. F. W. J. Teale; *Photochemistry and photobiology*, **10**, 363 (1969)

83. J. Eisinger, J. Flores, W. P. Petersen; *Biophys. J.* **49**, 987 (1986)

84. S. Tsuneda, T. Endo, K. Saito, K. Sugita, K. Horie, T. Yamashita, T. Sugo; *Chem. Phys. Lett.*, **275**, 203 (1997)

85. R. C. weast (Ed.); "*CRC-Handbook of Chemistry and Physics"*, 62nd Ed., CRC-Press inc. Boca Raton (1981)

86. D'ans Lax, *Tachenbuch für Chemiker und Physiker*, 1st Band, 3rd Auflage (1968)

87. M. Hollas; *Dissertation*, TU Clausthal (1999)

88. D. Myers; *Surfaces, Interfaces and colloids*, VCH Publisher: Weinheim (1990)

89. S. F. Scarlata and J. A. Ors; *polymer communication*, **27**, 41, (1986)

90. K. M. Abedin, J. Y. Ye, H. Inouye, T. Hattori, H. Sumi and H. Nakatsuka; *J. Chem. Phy.*, **103**, 15, (1995)

91. K. Nakashima, T. Anzai and Y. Fujimoto; *Langmuir*, **10**, 658, (1994)

92. T. Nivaggioli, B. Tsao, P. Alexandridis and T. A. Hatton; *Langmuir*, **11**, 119 (1995)

93. M. Canva, G. Le Saux, P. Georges, A. Brun, F. Chaput and J. P. Boilot; *Chem. Phys. Lett.*, **176**, 45, (1991)